Mon. Not. R. Astron. Soc. **327,** 353–368 (2001)

Rotational mixing in early-type main-sequence stars

Ian D. Howarth★ and Keith C. Smith†
Department of Physics and Astronomy, University College London, Gower Street, London WC1E 6BT

Accepted 2001 May 17. Received 2001 May 17; in original form 2000 November 21

ABSTRACT

We present quantitative observational investigations into the importance of rotationally induced mixing in late-O stars. First, we conduct non-LTE, hydrostatic, plane-parallel H/He model-atmosphere analyses of the optical spectra of three of the most rapidly rotating late-O near-main-sequence stars known: HD 93521 (O9.5 V), HD 149757 (ζ Ophiuchi; O9.5 V), and HD 191423 (ON9 III: n), all of which have equatorial rotation velocities of $\sim 430\,\mathrm{km\,s^{-1}}$ and $\omega_e/\omega_e(\mathrm{crit}) \simeq 0.9$. The analysis allows for the expected (von Zeipel) variation of T_{eff} and $\log g$ with latitude. These three stars are found to share very similar characteristics, including substantially enhanced surface-helium abundances ($y \simeq 0.2$). Secondly, we compare the distribution of projected rotational velocities for ON and morphologically normal dwarf O stars, and demonstrate that the ON stars are drawn from a population with more rapid rotation. The results provide qualitative support for rotationally induced mixing, although there remain discrepancies between atmospheric and evolutionary models (which we show employ inappropriate mass-loss rates for late-O main-sequence stars). We show that the most rapid rotator known, HD 191423, is an ON star, and note the implied disparity between O/ON morphology and surface helium abundance; we discuss consequences for the interpretation of spectral morphology in O-type main-sequence stars. We demonstrate a new, purely spectroscopic, method of distance determination for rapid rotators, and thereby confirm that HD 93521 lies at ~ 2 kpc, and is not, as previously suggested, a low-mass Population II star. Finally, our models contradict earlier claims of strongly differential surface rotation, and are consistent with uniform angular velocity at the surface.

Key words: stars: early-type – stars: evolution – stars: individual: HD 93521 – stars: individual: ζ Ophiuchi – stars: individual: HD 191423 – stars: rotation.

1 INTRODUCTION

Observations of the physical and chemical properties of massive stars ($\gtrsim 10\,\mathrm{M}_\odot$) offer powerful constraints on, and continuing challenges to, models of stellar structure and evolution. One such challenge is the observational evidence that the products of nucleosynthesis may be exposed in the photospheres of such stars during core hydrogen burning; this is contrary to 'traditional' evolutionary models, which predict no mixing of core-processed material to the surface layers of massive stars until they have evolved to the red part of the Hertzsprung–Russell diagram (e.g. Schaller et al. 1992).

There are two particularly well-established lines of evidence for the exposure of processed material during main-sequence phases in the upper Hertzsprung–Russell diagram. First, a small number of $\sim$ O9–B1 main-sequence stars[1] show the ratio of N III λ4640/C III λ4650 line blends to be anomalously large for their spectral types, as defined by the helium lines or the helium/silicon reference frame (Walborn 1976). The line-strength behaviour is strongly (but only qualitatively) suggestive of enhanced nitrogen:carbon abundance ratios in these OBN stars, and thus of the exposure of CNO-processed material.

A second photospheric indicator of mixing is the presence of surface helium abundances apparently enhanced above the standard solar, or cosmic, value. This result is again in conflict with the predictions of traditional evolutionary models. Herrero et al. (1992) studied this effect, which they labelled the 'helium

★E-mail: idh@star.ucl.ac.uk
† Deceased 2000 June 3.

[1] The assignment of a supergiant luminosity class to an O-type star is based solely on spectral morphology, not evolutionary status; O supergiants are, probably, 'main-sequence' stars in an evolutionary sense, i.e. are core hydrogen burning. We adopt the classification convention throughout this paper: 'main sequence' is to be read as equivalent in meaning to luminosity class V.

discrepancy', in the spectra of 25 Galactic O stars. Their homogeneous analysis of a comparatively large sample clarified several results which, although previously reported in the literature (e.g. Voels et al. 1989), had not been securely identified as systematic trends; in particular, Herrero et al. found near-solar surface helium abundances for slowly rotating O dwarfs, but enhanced helium in morphologically normal O supergiants.

These observations, among others (e.g. Gies & Lambert 1992; Fliegner, Langer & Venn 1996), have prompted a number of investigations into the role of rotationally induced mixing in the evolution of massive stars (e.g. Heger & Langer 2000; Maeder & Meynet 2000b, and references therein). However, while it seems beyond doubt that such mixing is an important factor in stellar evolution, the observational basis, although extensive, is still open to critical scrutiny. For example, the 'helium discrepancy' appears to be almost ubiquitous in the low-gravity supergiants, but becomes generally negligible in higher-gravity dwarfs. This suggests the possibility that the helium discrepancy may arise, at least in part, as a result of shortcomings in the atmospheric models which become more acute at lower gravities. (Such shortcomings most probably account for the 'mass discrepancy', also reported by Herrero et al. 1992.) This point is emphasized by work which shows that the inclusion of microturbulence in radiative-transfer models can alleviate the helium discrepancy in some regions of $T_{\rm eff}$, $\log g$ parameter space (McErlean, Lennon & Dufton 1998; Smith & Howarth 1998; Villamariz & Herrero 2000). Countering this argument is Herrero et al.'s finding that the helium discrepancy increases with increasing rotation for O dwarfs; the analysis of slowly and rapidly rotating O dwarfs is, superficially, a 'like with like' comparison, and should therefore yield reliable differential helium abundances, even if there are systematic errors in the absolute values. However, the most rapidly rotating stars are expected to show important variations in surface gravity and temperature as a function of latitude, which have not been properly allowed for in previous analyses. We address this deficiency in the present paper, with a new analysis of three very rapidly rotating late-O main-sequence (or near-main-sequence) stars: HD 93521, HD 149757 (ζ Oph), and HD 191423.

A further concern arises because the limitation of the 'N' qualifier to, generally, late-O/early-B types is largely a selection effect, resulting from the weakness of the defining lines in later types together with the strong temperature and, particularly, luminosity dependence of those lines at earlier types. A corollary of this is that it is not beyond question that the exceptional spectral morphology of OBN stars is attributable to subtle differences in atmospheric structure, rather than chemical composition. This possibility was recognized by Walborn (1976), and is further discussed by Mathys (1988), who notes in particular a general lack of correlation in late-O dwarfs between the defining N III λ4640 blend and N III λ4514, which has been proposed as an alternative morphologically based indicator of chemical processing (Bisiacchi, Lopez & Firmani 1982); Grigsby, Morrison & Anderson (1992) also note 'puzzling' inconsistencies in the behaviour of the carbon and nitrogen spectra of late-O and early-B main-sequence stars. Of course, this issue could in principle be resolved by quantitative analyses, but to date the optical CNO spectra of early-type stars have proven to be resistant to satisfactory modelling. For example, although Schönberner et al. (1988) found evidence to support the view that the morphological characteristics primarily reflect underlying abundance anomalies, they were forced to make an ad hoc selection of 'good' lines, and our own unpublished work is in agreement; even line-blanketed non-LTE models have failed to give satisfactory agreement with observations (Grigsby et al. 1992). We attempt a more model-independent investigation of the nature of ON stars in the present paper, by studying the distribution of rotational velocities in late-O main-sequence stars.

2 OBSERVATIONS

Rotational mixing is expected to increase in importance with increasing mass (Maeder 1998), and so O-type stars are the most favourable targets for study in this context (the availability of helium spectra in two stages of ionization being a further advantage). Our spectroscopic study is therefore based on three of the most rapidly rotating O-type stars known.

(i) *HD 93521.* Extensive time-series observations of HD 93521 were obtained over the course of four nights in 1994 March with the Utrecht Echelle Spectrograph (UES) on the 4.2-m William Herschel Telescope (WHT). These have been averaged into a single spectrum covering the wavelength range 4535–6800 Å at a resolving power of $R \simeq 3 \times 10^4$ (degraded from the instrument's intrinsic capability as a result of on-chip binning). Three additional observations with the same instrument were obtained from the Isaac Newton Group (ING) archive, and cover the spectral range from the Balmer limit to Hα at $R \simeq 10^5$, at somewhat poorer signal to noise ratios. Intermediate-dispersion spectra at $R \simeq 3500$, covering a similar wavelength range, were also obtained, with the WHT's ISIS cassegrain spectrograph, primarily as an aid to rectification and continuum placement in the echelle data.

(ii) *HD 149757.* HD 149757 was observed with UES in 1994 March, during the HD 93521 time-series run, with the same setup. Two further echellograms were obtained from the ING archive, to extend wavelength coverage. To assist in rectification and continuum placement, we used a range of supplementary observations: ISIS spectra obtained in 1992, 1994 and 1998 (accompanied by 'quick-look' red spectra to check for emission at Hα emission, which was never present); the Isaac Newton Telescope (INT) observations reported by Herrero et al. (1992), obtained from the ING archive; and the means of spectra obtained at Dominion Astrophysical Observatory (DAO) and Kitt Peak National Observatory (KPNO) discussed by Reid et al. (1993).

(iii) *HD 191423.* Only ISIS spectra are available for HD 191423, obtained in 1998 August with a 600B grating. These data cover the range $\sim$ 3950–5650 Å at a signal to noise ratio of $\sim$ 300 (falling off at the ends of the coverage, because of vignetting) and $R \simeq 4000$. This resolution adequately resolves the lines for such a rapid rotator.

All observations were extracted by using standard procedures, implemented in ECHOMOP (Mills, Webb & Clayton 1997), the only additional step we have taken being initial rectification of the UES data by fitting 2D polynomial surfaces to the echellograms.

3 SPECTRUM SYNTHESIS: MODELS

3.1 Procedure

The spectrum synthesis is performed simply by dividing the model stellar surface into a large number of facets and evaluating $T_{\rm eff}$ and $\log g$ at the centre of each facet. The flux emitted in the direction of the observer for this $T_{\rm eff}$, $\log g$ is interpolated from a grid of model atmospheres, shifted by the projected velocity of the facet, and added into the summed spectrum, which is weighted by the projected area of the facet. The approach is by no means novel (cf.

for example Collins 1963; Collins & Harrington 1966; Stoeckley 1968; Hardorp & Strittmatter 1968), but has not been widely applied using non-LTE models.

3.2 Geometry

The geometry of the photosphere is assumed to be given by a time-independent equipotential surface, constructed by adopting a simple Roche, or point-mass, model; the Roche approximation is justified by reference to polytropic models (Plavec 1958; Martin 1970), which show that more realistic mass distributions lead to negligible changes in the shapes of the equipotential surfaces. With this approximation the potential is

$$-\psi = GM_*/R(\theta) + \omega^2(\theta)(x^2 + y^2)/2 \tag{1}$$

in a coordinate system centred on a star of mass M_*, where $x^2 + y^2 \equiv [R(\theta)\sin\theta]^2$, θ is the colatitude, and ω is the angular velocity; the direction of increasing x is arbitrary because of axial symmetry.

The surface is defined by specifying $GM_*/R(\theta)$ at any reference point (we choose the pole), together with the equatorial angular velocity. In order to retain flexibility (cf. Section 5), we choose a simple rotation law for which the centrifugal force is conservative:

$$\omega(\theta) = \omega_e\{1 - F + F[R(\theta)\sin(\theta)/R_e]^2\}, \tag{2}$$

where F characterizes the differential surface angular rotation and the 'e' subscripts denote equatorial values. In hydrostatic equilibrium the pressure gradient is

$$\nabla P = \rho\nabla\psi; \tag{3}$$

because ρ is scalar, $P = P(\psi)$, so that equipotential surfaces are also surfaces of constant pressure. Thus the limiting case $F = 0$ (no differential surface rotation) is equivalent to constant angular velocity on an isobar, and therefore corresponds to 'shellular rotation', discussed by Zahn (1992) and widely adopted in studies of stellar evolution including rotation (e.g. Meynet & Maeder 1997; Denissenkov, Ivanova & Weiss 1999; Heger, Langer & Woosley 2000).

The geometry and stellar mass determine the Newtonian surface gravity at any point, $\boldsymbol{g} = \nabla\psi$; with the polar temperature and gravity as given model parameters, the variation of local temperature, T_ℓ, across the surface is characterized by assuming

$$T_\ell/T_p = (g_\ell/g_p)^{0.25}, \tag{4}$$

where g is the magnitude of $\boldsymbol{g}$ and the 'p' subscripts denote polar values. Equation (4) is von Zeipel's law of gravity darkening (von Zeipel 1924; Kippenhahn & Weigert 1990) and is discussed further in Section 3.4.

3.3 Fit parameters

In a standard model atmosphere analysis, there are three free model parameters: the effective temperature, $T_{\rm eff}$; the Newtonian surface gravity, $\log g$; and the helium abundance by number, $y = n(\mathrm{He})/[n(\mathrm{H}) + n(\mathrm{He})]$. To this list we may add ξ, the microturbulent velocity, often taken to be zero in non-LTE analyses (Becker & Butler 1989). In our models of rotating stars, we assume that y and ξ are independent of location on the surface. (This assumption is qualitatively justified by noting that horizontal mixing dominates over vertical mixing in Zahn's picture.) For convenience, we use the polar temperature, T_p, and the polar gravity, $\log g_p$, as fit parameters, in place of the conventional $T_{\rm eff}$ and $\log g$.

To specify a rotating-star model fully we require four further parameters,[2] one of which is the rotation-law parameter, F (equation 2). Although other combinations of variables may be used, the remaining parameters can conveniently be selected to be the equatorial rotation velocity, v_e; the inclination of the rotation axis to the line of sight, i; and the ratio $\omega_e/\omega_e(\mathrm{crit})$, where the critical angular rotation velocity at which the equatorial effective gravity is zero is given by

$$\omega_e(\mathrm{crit}) = v_e(\mathrm{crit})/R_e(\mathrm{crit}) = \sqrt{[GM_*/R_e^3(\mathrm{crit})]} \tag{5}$$

and where $R_e(\mathrm{crit}) = 1.5R_p$. It may be noted that $\omega_e/\omega_e(\mathrm{crit}) \neq v_e/v_e(\mathrm{crit})$, because of the dependence of R_e on v_e; and that for strongly differential surface rotation and high rotation rates, it is possible for the effective gravity on an equipotential to be positive at the equator but not at some higher latitudes.

3.4 von Zeipel's 'law'

For a given rotation parameter F and normalized rotation rate $\omega_e/\omega_e(\mathrm{crit})$, von Zeipel's law enforces a unique relationship between the polar temperature, T_p, the equatorial temperature, T_e, and the effective temperature,

$$T_{\rm eff}^4 = \int T_\ell^4\,\mathrm{d}A \Big/ \int \mathrm{d}A \tag{6}$$

(where A is the surface area). This relationship, and the dependences of various equatorial quantities on rotation, are illustrated for $F = 0$ in Fig. 1; while the equatorial temperature formally approaches zero as rotation approaches critical, the effective temperature asymptotes to $\sim 0.8T_p$. Maeder (1999) has considered modifications to von Zeipel's law in the case of differential rotation, and finds only small differences from equation (4).

As long as von Zeipel's law applies, radiation pressure has no important effect on the surface geometry (equation 1), because the ratio of inward gravity to outward radiation pressure is then independent of θ (for fixed flux-mean opacity), both varying as T_ℓ^4. Clearly, von Zeipel's law cannot apply rigorously; it requires that hydrostatic and radiative equilibria apply simultaneously in the envelope, and von Zeipel (1924) showed that this situation cannot hold in a rotating star. This has led to a dichotomy in the recent literature as to whether the critical rotation velocity is significantly modified by radiation pressure (Langer 1998, Lamers et al. 1999) or not (Howarth & Reid 1993, Howarth 1997; Glatzel 1998; Meynet & Maeder 2000).

There are several observational indications suggesting that von Zeipel's law is a good approximation in practice [and hence that the surface geometry, and $v_e(\mathrm{crit})$, are insensitive to radiation-pressure effects]. First, the most rapid rotators exhibit projected equatorial velocities which approach $v_e(\mathrm{crit})$ (e.g. Slettebak 1966; Hardorp & Strittmatter 1968; Porter 1996; this paper), which would not be the case if equatorial radiation pressure played a major role. Secondly, rapidly rotating late-O non-radial pulsators show larger amplitudes of variability in He I than He II lines – evidence for equatorially confined sectoral modes with the equator cooler than the poles (Howarth & Reid 1993). Thirdly, photometric observations of binary systems require 'gravity darkening', and are

[2] Standard analyses have only one further, optional, parameter: $v_e \sin i$.

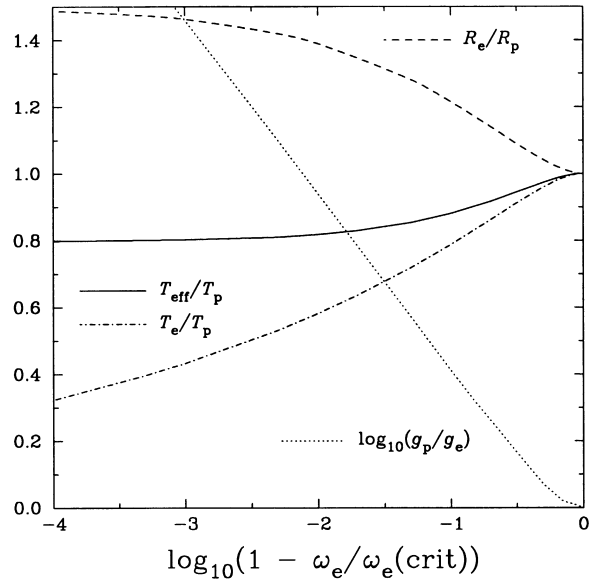

Figure 1. The ratios of equatorial gravity, effective temperature, equatorial temperature and equatorial radius to the polar values as a function of normalized equatorial rotation rate. Effective temperatures are shown for $F = 0$ (i.e. surface angular velocity constant).

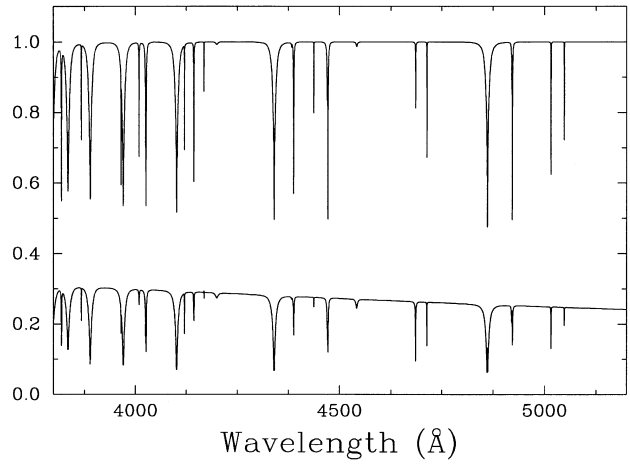

Figure 2. Limb-darkening is strongly variable through absorption lines in early-type stars. The upper plot shows the rectified flux spectrum for a $T_{\rm eff} = 30\,$kK, $\log g = 4.0$, $y = 0.09$, $\xi = 0\,\mathrm{km\,s^{-1}}$ model while the lower plot shows the linear limb-darkening coefficient u evaluated between $\cos\mu = 1.0$ and 0.5, where $I(\mu) = I(0) - u + u\cos\mu$ and μ is the viewing angle measured from the surface normal. (Note however that a linear limb-darkening law is not a particularly good approximation to our model atmospheres and is not assumed in constructing our model spectra.)

quantitatively consistent with the exponent in equation (4) (Rafert & Twigg 1980). Fourthly, there is direct, model-independent, evidence for gravity darkening in the present observations: in the echelle spectra of HD 93521 and HD 149757, the He I lines are measurably broader at half-depth than the He II lines, with λ4921 being slightly more than ~ 10 per cent wider at half-depth than λ4686, for example. Although there are hints of an asymmetry suggestive of stellar-wind contamination in λ4686 (see Fig. 6) there is no associated velocity displacement, so the simplest interpretation of the observations is that He I line formation is relatively favoured in cooler, more rapidly rotating equatorial regions.

3.5 Atmospheres

We use the grid of hydrostatic, plane-parallel, H/He, non-LTE model atmospheres described by Smith & Howarth (1998). These model atmospheres, generated by using TLUSTY (Hubeny & Lanz 1995), incorporate essentially the same physics as employed by Herrero et al. (1992).

Given locally specified values of temperature and gravity, together with global values for y and ξ, we interpolate in the grid of atmospheres for the emergent intensity as a function of wavelength, λ. We explicitly interpolate in emergent intensity as a function of viewing angle, rather than apply a simple limb-darkening law to flux data, because the limb-darkening is strongly variable through the lines (Fig. 2), although in practice the nett effect on the integrated spectrum is actually quite small.

3.6 Distance determination

Among other variables, the spectroscopic analysis constrains both $\omega_e/\omega_e(\mathrm{crit})$ and $\log g_p$. As

$$\omega_e/\omega_e(\mathrm{crit}) \propto \sqrt{v_e^2 R_p/M_*} \qquad (7)$$

and

$$g_p \propto M_*/R_p^2, \qquad (8)$$

we have estimates for two quantities which have different dependences on the three variables v_e, R_p, and M_*. We can therefore use these two quantities to obtain R_p and M_* (as we measure $v_e \sin i$ and can infer i, either from the spectroscopic analysis or from other considerations); with T_p we then obtain $M(V)$. In other words, if a star is rotating sufficiently close to its critical rotation velocity that its emergent spectrum is modified in an identifiable manner (which implies $\omega_e/\omega_e(\mathrm{crit}) \gtrsim 0.8$; Fig. 1), its distance and mass can be determined from a *purely spectroscopic* analysis.

This new method of mass and distance determinations is analogous to the well-documented technique of combining $\log g$ with the stellar wind mass-loss rate or terminal velocity, each of which again has a different functional dependence on M_* and R (e.g. Ebbets & Savage 1982; Kudritzki et al. 1992). Unfortunately, it suffers essentially the same drawback: the limited precision with which $\log g$ and $\omega_e/\omega_e(\mathrm{crit})$ can be determined means that the method will rarely be competitive with traditional approaches (such as simple spectroscopic parallax). However, as we shall demonstrate in the following discussions of individual stars, useful constraints can be obtained in some cases or, alternatively, known absolute magnitudes can be used to improve estimates of R_p and M_*.

4 SPECTRUM SYNTHESIS: ANALYSIS

We follow the normal approach, beginning with a coarse equivalent-width analysis using 'fit diagrams' (cf. for example Herrero et al. 1992; Smith & Howarth 1998). For each helium line contributing to the analysis (and we use all lines available to us at wavelengths < 6000 Å) a diagnostic track is determined, for which the model equivalent width matches the observed equivalent width

in the $T_{\rm eff}$, $\log g$ plane. For each Balmer line, the track is defined by locating, at each $T_{\rm eff}$, the $\log g$ which minimizes the sum of the squares of the differences between the model and the wings of the observed profile. The point about which the ensemble of tracks has a minimum dispersion is then selected as representing the best-fitting pair of atmospheric parameters. For a non-rotating, or slowly rotating, star, such fit diagrams represent a slice-through three-dimensional $T_{\rm eff}$, $\log g$, y space (with ξ as a potential fourth dimension); several such slices at different values of y are therefore compared to determine the best-fitting helium abundance. The parameters are then 'tuned' by a fine analysis, wherein the model line profiles are directly compared to observations.

The rotating-star case introduces significant additional dimensionality. To minimize the extent of parameter space to be explored from the outset, we assume $F = 0$ (i.e. ω independent of θ), except as noted in Section 5. Fit diagrams in the $T_{\rm p}$, $\log g_{\rm p}$ plane are constructed by specifying y, $\omega_{\rm e}/\omega_{\rm e}({\rm crit})$ and i. This combination of parameters is sufficient to generate model equivalent widths which are independent of $v_{\rm e}$ (other than through blending effects), although, of course, a fine analysis requires this quantity – a simple rotational convolution of the flux spectrum will not give correct results for a star where temperature and gravity vary significantly over the stellar surface.

In the initial coarse analysis, we examine fit diagrams for $\log g_{\rm p} = 3.3$–4.5, $T_{\rm p} = 30$–$44\,{\rm kK}$ at $\omega_{\rm e}/\omega_{\rm e}({\rm crit}) = 0.05, 0.5, 0.8, 0.9, 0.95$ and 0.98, and $y = 0.09, 0.2, 0.3$. (As discussed below on a star-by-star basis, we can reduce the dimensionality of the problem by using independent data to constrain i to better accuracy than can be obtained from the spectra.) At each slice in this four-dimensional space we estimate the value of $\omega_{\rm e}/\omega_{\rm e}({\rm crit})$ which minimizes the dispersion about the best-fitting $T_{\rm p}$, $\log g_p$ pair, and from this set of solutions we select the y-value which globally minimizes that dispersion. The final parameters are adopted on the basis of adjustments following line-profile fits.

The selection of the 'best' solutions could, in principle, be achieved by purely objective criteria; Smith & Howarth (1998) took a step in this direction by choosing the point which minimizes the rms of the (scaled) orthogonal distances to the collection of diagnostic tracks. However, such objective techniques (and the formal error estimates which they are capable of providing) are most useful only when the model provides a satisfactory simulation of the data, in the sense that the model profiles match the data to within the observational errors for all lines. Unfortunately, this is not the case for the simple models used here, where omitted physics, such as line blanketing, results in significant residual differences between the best-fitting profiles and the data for at least some lines (see e.g. discussions by Voels et al. 1989; Herrero et al. 1992; Lennon 1994; Smith & Howarth 1994, 1998; Herrero, Puls & Villamariz 2000; Villamariz & Herrero 2000). Our estimates of $T_{\rm p}$, $\log g_{\rm p}$, y, etc. must therefore be interpreted simply as the set of numerical values that generate the model which is subjectively judged to provide the best match to a given spectrum (and not, necessarily, the physical values relevant to that spectrum). Similarly, the error estimates should be interpreted as reflecting the total ranges over which the model fits remain acceptable by comparison to the best-fitting model.

4.1 HD 214680 (10 Lac): a standard star

10 Lac is an O9 V standard (Walborn 1973) with unusually narrow lines for an O-type star ($v_{\rm e} \sin i \simeq 35\,{\rm km\,s^{-1}}$; Howarth et al. 1997). Although the narrowness of the lines may be caused in part by the viewing angle, it is unlikely that the intrinsic rotation is *very* rapid; e.g. $v_{\rm e} > 200\,{\rm km\,s^{-1}}$ would require $i \lesssim 10°$.

This star has been analysed with non-LTE models by several groups (Schönberner et al. 1988; Grigsby et al. 1992; Herrero et al. 1992), all of whom find essentially solar helium abundances. We conducted our own analysis (of a UES spectrum) as a check that our grids do not lead to inconsistent helium abundances through any computational or procedural errors.

A coarse analysis yields $T_{\rm eff} = 39\,{\rm kK}$, $\log g = 4.1$, $y = 0.09$, with estimated uncertainties of 1 kK, 0.1 and 0.02, respectively. For comparison, Schönberner et al. give 38 kK, 4.25 and 0.09; Herrero et al. report 37.5 kK, 4.0 and 0.10; and Grigsby et al. find 30 kK and 4.0 for an assumed $y = 0.10$. The Grigsby et al. temperature estimate, based on line-blanketed models, is significantly lower than that found by other authors. Grigsby et al. suggest that this is a consequence of Schoñberner et al. using He II λ4686, but in our analysis (and that of Herrero et al.) this line is well matched by the same model as is required to fit other lines; a more likely explanation is that line-blanketed hot-star models generally appear to give cooler effective temperatures than unblanketed models (Hubeny, Heap & Lanz 1998).

We conclude that our models are consistent with those used by previous analysts, and in particular yield the expected solar helium abundance for 10 Lac.

4.2 HD 93521

HD 93521 is an O9.5 V star (Hobbs et al. 1982) with a number of unusual characteristics, including high galactic latitude, and anomalous and time-variable line profiles consistent with non-radial pulsation (Fullerton, Gies & Bolton 1991; Massa 1992; Howarth & Reid 1993). It is one of the most rapidly rotating stars known, with $v_{\rm e} \sin i$ estimates of 341, 400, 400 and 432 $\,{\rm km\,s^{-1}}$ in the literature (Penny 1996; Conti & Ebbets 1977; Lennon et al. 1991; Howarth et al. 1997).

We focus our attention on models with $i = 90°$, based in part on the exceptionally rapid rotation, but primarily on the interpretation of ultraviolet (UV) resonance-line profiles in terms of a vertically thin equatorial disc, viewed edge-on (Massa 1992; Howarth & Reid 1993; Bjorkman et al. 1994). With this restriction, the rotating-star models have only one more free parameter than traditional fits: $\omega_{\rm e}/\omega_{\rm e}({\rm crit})$. The adopted best-fitting parameters at $i = 90°$ are $T_{\rm p} = 38 \pm 1.5\,{\rm kK}$ and $\log g_{\rm p} = 3.9 \pm 0.1$, with $\omega_{\rm e}/\omega_{\rm e}({\rm crit}) = 0.9$ ($T_{\rm eff} = 33.5\,{\rm kK}$, $\log g_{\rm e} = 3.5$) and with an adopted value of $v_{\rm e} \sin i = v_{\rm e} = 435\,{\rm km\,s^{-1}}$ (rounded up from Howarth et al. 1997). Varying $\omega_{\rm e}/\omega_{\rm e}({\rm crit})$ by $^{+0.05}_{-0.10}$, which covers the range of tolerable solutions, changes the best-fitting $T_{\rm p}$ by $\sim \pm 2\,{\rm kK}$ and $\log g_{\rm p}$ by $\sim \pm 0.2$; $T_{\rm eff}$ is almost unchanged. The inferred temperature and polar gravity are insensitive both to the helium abundance and to microturbulence.

We find that no model with solar helium abundance gives a satisfactory fit to the data, a result which remains true irrespective of assumed inclination (and already indicated, on the basis of simpler models, by Hack & Yilmaz 1977 and by Lennon et al. 1991). The dispersion in the fit diagram is minimized at $y = 0.20$ if we assume zero microturbulence; a marginally better match to observations is obtained with $\xi = 10\,{\rm km\,s^{-1}}$, which yields $y = 0.16$. We adopt $y = 0.18 \pm 0.03$.

The observations are compared with a model spectrum in Fig. 3; the corresponding $y = 0.09$ model is also shown to demonstrate that an enhanced helium abundance is required if the model is to reproduce the observed spectrum satisfactorily. In the parameter

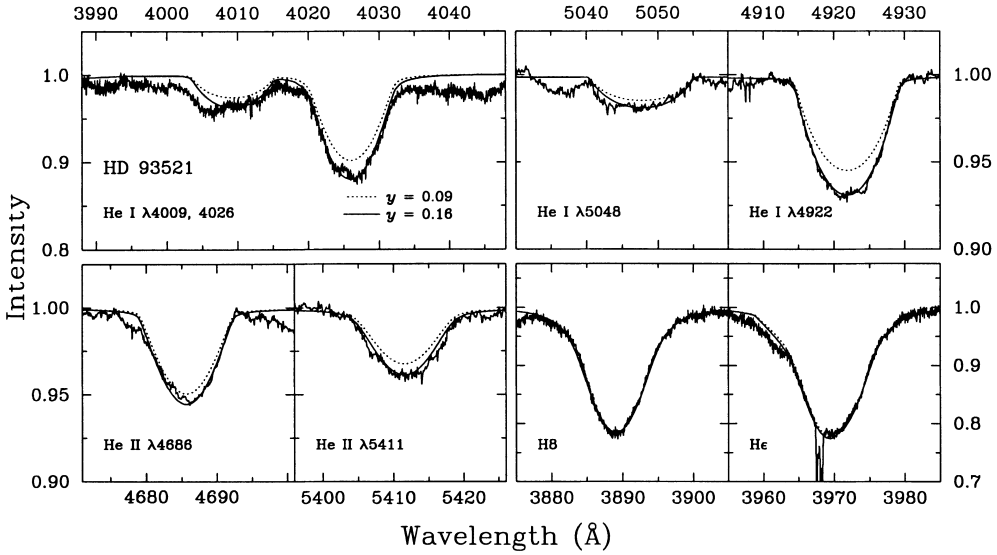

Figure 3. Comparison of H/He lines in the spectrum of HD 93521 with a model characterized by $i = 90°$, $\xi = 10\,\mathrm{km\,s^{-1}}$, $y = 0.16$, $T_\mathrm{p} = 38\,\mathrm{kK}$, $\log g_\mathrm{p} = 3.9$ and $\omega_\mathrm{e}/\omega_\mathrm{e}(\mathrm{crit}) = 0.90$ (solid line). The lower members of the Balmer series give poorer agreement between models and observations (cf. Section 4.2). The dotted line shows a model with $y = 0.09$ (but otherwise identical parameters) to illustrate the requirement for a model with enhanced helium abundance. The illustrated helium lines were selected more or less arbitrarily being well-observed in all the stars studied.

space of interest, the He II line-strengths are only weakly dependent on gravity, while the He I lines are dependent on both T_p and $\log g_\mathrm{p}$; thus for given values of $\omega_\mathrm{e}/\omega_\mathrm{e}(\mathrm{crit})$ the gravity can be constrained from the helium lines alone. The resulting model is in good agreement with the high members of the Balmer series, as illustrated in Fig. 3, but matches the lower members very poorly, being systematically broader and shallower than the observations. We attribute this to the effects of circumstellar material; Irvine (1989) and Howarth & Reid (1993) show that Hα is variable (with amplitudes and time-scales greater than the more subtle changes associated with the non-radial pulsation of the star) and shows emission wings. At the time of the observations shown in Fig. 3, the Hα profile again had emission wings, with central absorption much narrower than the adjacent He I λ6678 line (full-widths at half depth ~ 360 and $560\,\mathrm{km\,s^{-1}}$, respectively; see fig. 1 in Irvine 1989, or fig. 9 in Howarth et al. 1997, for illustration). This infilling of the Balmer lines evidently continues to play a role at least as far as Hδ.

The adopted model yields $L = 5.1\,\mathrm{dex\,L_\odot}$, $M(V) = -4.7$ (whence $D = 2.2\,\mathrm{kpc}$), $M_* = 27\,\mathrm{M_\odot}$, $R_\mathrm{p} = 9.7\,\mathrm{R_\odot}$. The uncertainty in T_p has only small consequences for $\log L$ and $M(V)$ (and none for M_*), but changing $\log g_\mathrm{p}$ by as little as ± 0.1 changes $\log L$ by $\sim\mp 0.2$, $M(V)$ by ± 0.5, and M_* by $\sim\mp 6\,\mathrm{M_\odot}$. More importantly, changing $\omega_\mathrm{e}/\omega_\mathrm{e}(\mathrm{crit})$ by $\pm^{0.05}_{0.10}$, while optimizing T_p and $\log g_\mathrm{p}$ [which correlate with $\omega_\mathrm{e}/\omega_\mathrm{e}(\mathrm{crit})$], changes $\log L$ by $\sim\mp 0.7$, M_V by $\sim\pm 1.5$, and M_* by $\sim\mp 0.4\,\mathrm{dex}$. However, even with these rather large uncertainties in the absolute parameters, our results securely rule out the possibility that HD 93521 is a $\sim$ solar-mass Population II object (cf. Ebbets & Savage 1982, and references therein). The best-fitting parameters found here are in excellent agreement with the illustrative model proposed by Howarth & Reid (1993), and thus support their conclusion that HD 93521 most probably formed well out of the Galactic plane.

4.3 HD 149757 (ζ Ophiuchi)

Zeta Oph has a spectral type of O9.5 V (Morgan, Code & Whitford 1955); it is the nearest and brightest of the very rapidly rotating O stars. Its ultraviolet P-Cygni profiles have unusual morphologies, including strong, high-velocity 'discrete absorption components' (Howarth et al. 1993), and are exceptionally well-developed for its spectral type. Massa (1995) has attributed these characteristics to a 'wind compressed disc' viewed at an intermediate angle. Two Hα emission-line episodes have been reported by Ebbets (1981), and the star is a non-radial pulsator (Vogt & Penrod 1983, Reid et al. 1993, Kambe et al. 1997).

We have searched for acceptable models with inclinations $i \geq 40°$. We find that zero-microturbulence models all require $\omega_\mathrm{e}/\omega_\mathrm{e}(\mathrm{crit}) \simeq 0.9 \pm 0.1$, $T_\mathrm{p} \simeq 39 \pm 2\,\mathrm{kK}$, $\log g_\mathrm{p} \simeq 4.0 \pm 0.2$, $y \simeq 0.2 \pm 0.03$ and $i \simeq 55$–$80°$. The parameters are correlated, with smaller values of $\omega_\mathrm{e}/\omega_\mathrm{e}(\mathrm{crit})$ requiring smaller values of T_p and $\log g_\mathrm{p}$ in order to match the observed line strengths. The model profiles are too narrow compared to observations if we use $v_\mathrm{e} \sin i = 370\,\mathrm{km\,s^{-1}}$ (from Howarth et al. 1997), so we adopt $v_\mathrm{e} \sin i = 400\,\mathrm{km\,s^{-1}}$, which is within the spread of values found in the literature [e.g. 348, 351, 390, 400 and $420\,\mathrm{km\,s^{-1}}$ according to Penny (1996), Conti & Ebbets (1977), Jankov, Janot-Pacheco & Leister (2000), Slettebak (1966) and Wallerstein & Wolff (1965), respectively], and in particular agrees well with other estimates based on direct profile fitting ($400\,\mathrm{km\,s^{-1}}$, Herrero et al. 1992; $400\,\mathrm{km\,s^{-1}}$, Puls et al. 1996; $390\,\mathrm{km\,s^{-1}}$, Balona & Kambe 1999).

A weakness of the spectroscopic method of distance determination described in Section 3.6 is the sensitivity of $M(V)$ to $\log g$ and $\omega_\mathrm{e}/\omega_\mathrm{e}(\mathrm{crit})$. In the case of HD 149757, we can turn this sensitivity to our advantage, because *Hipparcos* has provided a reliable parallax: $\pi = 7.12 \pm 0.71\,\mathrm{mas}$ (ESA 1997), which gives $M(V) = -4.2 \pm 0.2$.[3] This provides a strong constraint on $\log g_\mathrm{p}$ ($\partial M(V)/\partial \log g_\mathrm{p} \simeq 5\,\mathrm{dex^{-1}}$). The locus of models which match the observed $M(V)$ is almost orthogonal to the loci of

[3] This number follows from $V = 2.57$, $(B - V) = +0.02$ (Moffet & Barnes 1979), assuming $(B - V)_0 = -0.3$, $R = 3.1$.

models matching the He II line strengths, while the He I and Balmer lines form a third family of constraints. Considering all three constraints, only a very limited range of parameter space gives acceptable agreement between models and observations.

The adopted best-fitting parameters are: $i = 70 \pm 10°$ ($v_e = 425\,\mathrm{km\,s^{-1}}$), $y = 0.20 \pm 0.03$, $T_p = 39 \pm 1\,\mathrm{kK}$, $\log g_p = 3.99 \pm 0.05$, and $\omega_e/\omega_e(\mathrm{crit}) = 0.90 \pm 0.03$. This model yields $T_{\mathrm{eff}} = 34.3\,\mathrm{kK}$, $\log g_e = 3.58$, $L = 4.96\,\mathrm{dex\,L_\odot}$, $M(V) = -4.2$, $M_* = 20.0\,\mathrm{M_\odot}$, and $R_p = 7.5\,\mathrm{R_\odot}$. The mass and radius are somewhat smaller than those estimated for HD 93521, because of the slightly smaller value of v_e and slightly larger value of $\log g$ used for HD 149757.

The model yields an equatorial radius of $9.1\,\mathrm{R_\odot}$, and an area-equivalent radius,

$$R_A = \sqrt{\int dA/(4\pi)}, \tag{9}$$

of $8.5\,\mathrm{R_\odot}$ (the volume-equivalent radius is essentially the same). The corresponding angular diameter is 0.55 mas, in agreement with the intensity-interferometer value of 0.51 ± 0.05 mas (Hanbury Brown, Davis & Allen 1974). Of course, this agreement is not independent of the adopted $M(V)$, but does provide a useful consistency check.

A comparison between observed and predicted line profiles is made in Fig. 4; it is notable that He I λ4026 is poorly matched. The locus of models which fit this line runs roughly parallel to the other He I lines in the T_p, $\log g_p$ plane but is displaced by $\sim +8\,\mathrm{kK}$ (or $-0.4\,\mathrm{dex\,cm\,s^{-2}}$), for all $\omega_e/\omega_e(\mathrm{crit})$ and y. Thus no model which matches λ4026 also matches the other He I lines. He II λ4686 exhibits a redwards 'shoulder', which is suggestive of contamination by stellar wind or other circumstellar emission. (The feature is also present in the DAO spectrum of HD 149757 shown by Reid et al. 1993 and the INT spectrum analysed by Herrero et al. 1992.) However, Hα was a symmetric, pure absorption profile at the time of these observations, and there is no significant bluewards displacement of the λ4686 absorption. Otherwise, the overall quality of the fit is similar to that found by Herrero et al. (1992). They did not take account of the variation in T_ℓ, $\log g_\ell$, although their model implies a similar range in those quantities as found here; this led to an ambiguity in their best-fitting model, which allowed for a helium abundance as low as solar. Our models require enhanced helium, in agreement with the preferred solution of Herrero et al. (as well as that adopted by Puls et al. 1996).

4.4 HD 191423

Walborn (1973) classified HD 191423 as O9 IIIn, to which we add the 'N' qualifier (see Section 4.4.1). It is the fastest rotator in the Penny (1996) and Howarth et al. (1997) catalogues, the two $v_e \sin i$ estimates (392 and $436\,\mathrm{km\,s^{-1}}$) agreeing to within their joint errors. We use $v_e \sin i = 435\,\mathrm{km\,s^{-1}}$ in our modelling. In general, the spectrum closely resembles that of HD 93521; in particular, the UV resonance-line profiles are strikingly similar, and share peculiarities not yet observed in any other star (Howarth et al. 1997). Accordingly, we adopt $i = 90°$, for the same reasons as in the case of HD 93521.

A satisfactory fit is obtained at $\omega_e/\omega_e(\mathrm{crit}) = 0.9$ for a model with $T_p = 39 \pm 1.5\,\mathrm{kK}$, $\log g_p = 3.8 \pm 0.1$. However, as with the other two rapid rotators considered here, there is near-degeneracy between parameter sets, in that reasonable fits can be obtained at smaller [larger] values of $\omega_e/\omega_e(\mathrm{crit})$ with smaller [larger] values of T_p and $\log g_p$. This degeneracy can, in principle, be broken by using observations of sufficiently high quality, although in practice the limiting factors are likely to be continuum placement and blending, not the signal to noise ratio or resolution. In any event, the degeneracy is certainly exacerbated by the poorer quality of the HD 191423 spectra compared with the echelle data available for the other two stars. We demonstrate the problem in Fig. 5 with two 'best-fitting' models having quite different values of $\omega_e/\omega_e(\mathrm{crit})$. The adopted model [and the illustrated $\omega_e/\omega_e(\mathrm{crit})$ 0.8, 0.95 models] has $T_{\mathrm{eff}} = 34.3\,\mathrm{kK}$ [33.5, 35.0], $\log L = 5.5\,\mathrm{dex\,L_\odot}$ [5.9, 5.0], $R_p = 13.6\,\mathrm{R_\odot}$ [24.7,7.0].

Once again, no model with solar helium abundance gives a satisfactory fit to the data; irrespective of $\omega_e/\omega_e(\mathrm{crit})$, best fits require $y \simeq 0.2$ at $\xi = 0\,\mathrm{km\,s^{-1}}$; using $\xi = 10\,\mathrm{km\,s^{-1}}$ has only a small effect, yielding $y \simeq 0.18$.

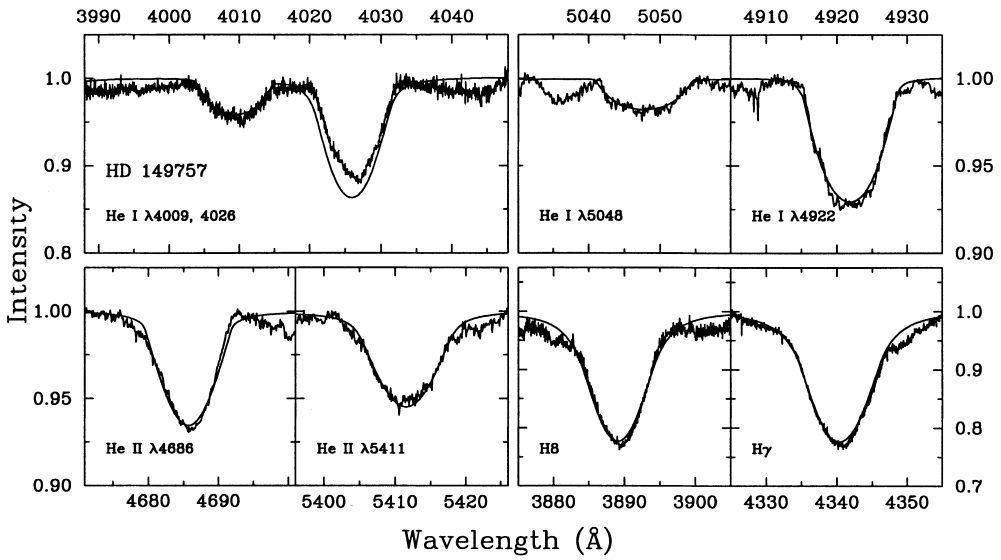

Figure 4. Comparison of selected H/He lines in the spectrum of HD 149757 with a model characterized by $i = 70°$, $\xi = 0\,\mathrm{km\,s^{-1}}$, $y = 0.20$, $T_p = 39\,\mathrm{kK}$, $\log g_p = 4.0$ and $\omega_e/\omega_e(\mathrm{crit}) = 0.90$. The He I λ4471 line is shown in Fig. 7.

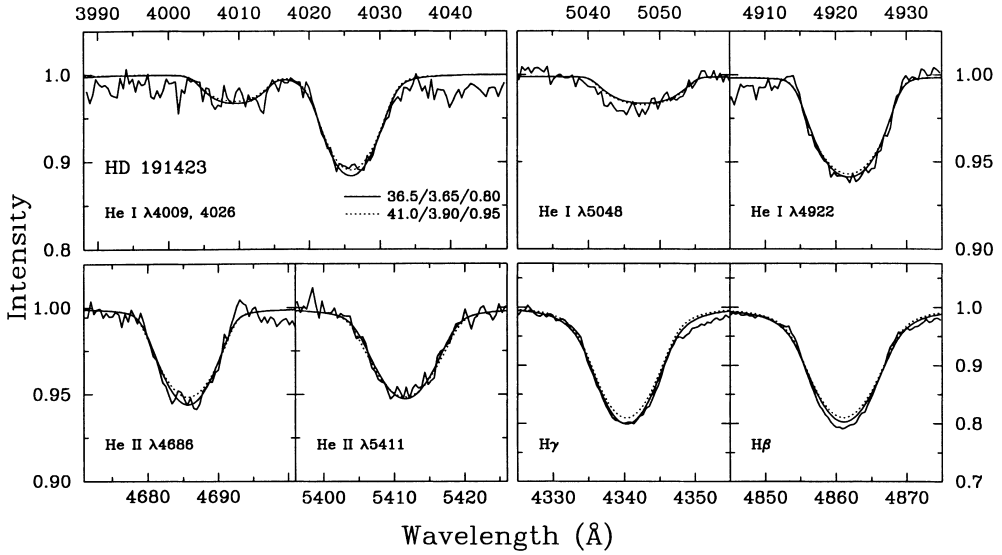

Figure 5. Comparison of selected H/He lines in the spectrum of HD 191423 and models with $i = 90°$, $\xi = 0\,\mathrm{km\,s^{-1}}$ and $y = 0.20$. The models are labelled with T_p, $\log g_\mathrm{p}$ and $\omega_\mathrm{e}/\omega_\mathrm{e}$(crit) (kK/dex cgs/dimensionless), and illustrate the near-degeneracy of solutions with different values of $\omega_\mathrm{e}/\omega_\mathrm{e}$(crit).

4.4.1 Spectral morphology

Although the spectrum of HD 191423 is generally very similar to that of HD 93521, there are important differences in the $\lambda\lambda$4640–4650 region, illustrated in Fig. 6. In spite of the severe blending resulting from rapid rotation, this figure clearly shows that the λ4650 C III blend is much weaker in HD 191423, and is comparable with line strengths in the ON star HD 201345. We conclude that HD 191423 is also an ON star according to the precepts described by Walborn (1976).

5 DIFFERENTIAL ROTATION?

Stoeckley & Buscombe (1987) conducted a study of HD 149757 (and 18 other rapidly rotating stars), using a modelling approach closely related to ours. They considered only the He I λ4471 and Mg II λ4481 lines, but employed an objective, least-squares technique to derive values for $v_\mathrm{e}\sin i$, an 'aspect parameter', $\{v_\mathrm{e}^2 - [v_\mathrm{e}\sin i]^2\}/\{v_\mathrm{e}^2(\mathrm{crit}) - [v_\mathrm{e}\sin i]^2\}$, and the differential rotation parameter F (equation 2). They found strongly differential rotation in HD 149757 (and nearly all other stars in their sample), with $F = -0.53\pm^{0.12}_{0.07}$; that is, they concluded that the polar regions have an angular velocity ~ 50 per cent greater than the equator (unlike the Sun, which has a polar angular velocity ~ 35 per cent smaller than the equatorial value).

As these results could have considerable importance for our analyses (and for the assumption of shellular rotation), we have constructed grids of models with $F = -0.5$ in order to investigate Stoeckley & Buscombe's result. We find that the computed equivalent widths are subject to only relatively minor changes as a result of differential rotation, all other parameters being held fixed, because the temperature and gravity at the equator and poles are independent of F with the formulation we have adopted. However, with negative values of F the rotation away from the equator is faster than it is with $F = 0$; in consequence, the surface gravity and temperature in temperate zones (in particular) are reduced, resulting in a small reduction in T_eff ($\lesssim$4 per cent for $F = -0.5$). Thus the line strengths of such a differentially rotating model are matched by those of a uniformly rotating model having only very slightly larger values of T_p and $\log g_\mathrm{p}$.

The effects on the line profiles, by contrast, are large; the fast temperate-zone rotation moves absorption away from the line centre and into the wings, resulting in much 'boxier' profiles. Such profiles are in considerably poorer agreement with observations than the $F = 0$ models adopted elsewhere in this paper; we illustrate this in Fig. 7, where our adopted model is shown together with the corresponding $F = -0.5$ calculation (where T_p has been increased to 39.6 kK to conserve T_eff). Also shown is the model based on Stoeckley & Buscombe's adopted parameters ($M_* = 20\,\mathrm{M_\odot}$, $R_\mathrm{p} = 10\,\mathrm{R_\odot}$, $T_\mathrm{eff} = 34.1$ kK, $v_\mathrm{e} = 423\,\mathrm{km\,s^{-1}}$, $i = 53°$, $y = 0.09$, and $\xi = 0$), as well as a second model with

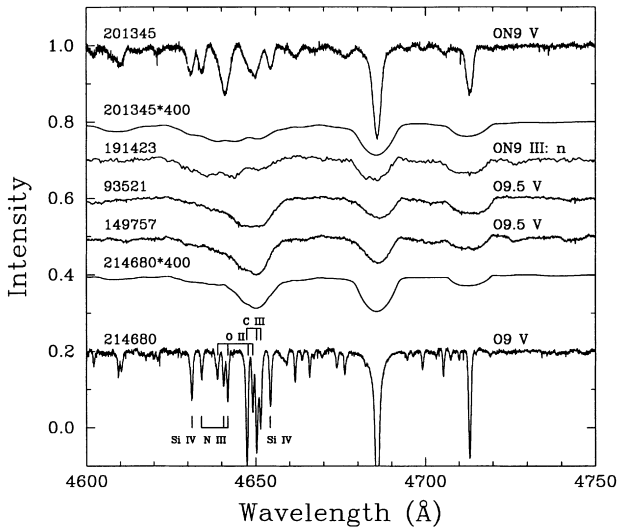

Figure 6. Spectra of rapid rotators and the relatively narrow-lined stars HD 201345 and 214680 ($v_\mathrm{e}\sin i = 91$ and 35 $\mathrm{km\,s^{-1}}$ according to Howarth et al. 1997). The spectra of the two slow rotators are shown again after convolution with a rotational broadening function having $v_\mathrm{e}\sin i = 400\,\mathrm{km\,s^{-1}}$. The principal contributors to the 4640–4650 complex are identified; the weakness of the C III lines in the spectrum of HD 191423 shows it to be an ON star.

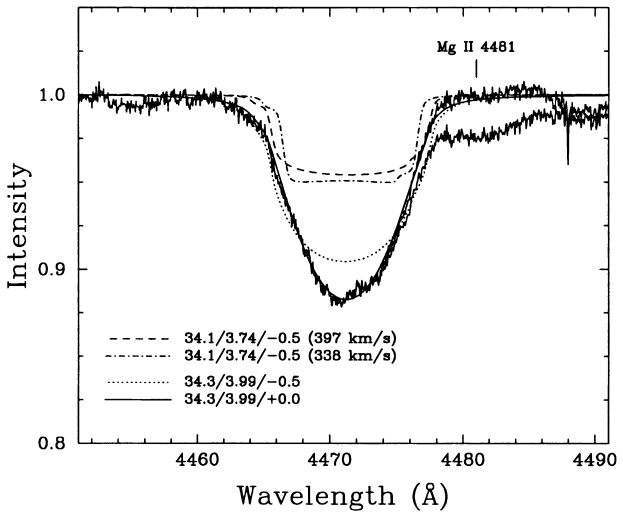

Figure 7. Comparison between the He I λ4471 line in the spectrum of HD 149757 and models incorporating differential rotation, labelled by $T_{\rm eff}/\log g_{\rm p}/F$ (kK/cgs/dimensionless). The 34.3/3.99/+0.0 model is the model adopted here, and is further illustrated in Fig. 4. The 34.1-kK models, additionally labelled with the relevant $v_{\rm e}\sin i$ value, are the basis of previous claims of evidence for differential rotation (cf. Section 5). The observed spectrum is shown as recorded, and with an approximate correction for the blended Mg II line obtained by division with a shifted, scaled copy of λ4471.

$i = 70°$, chosen to reproduce the value of $v_{\rm e}\sin i$ adopted here. The implied value of $\omega_{\rm e}/\omega_{\rm e}({\rm crit})$ is 0.963, with $\log L = 5.32\,{\rm dex\,L_\odot}$ (the latter figure disagreeing with Stoeckley & Buscombe's published value because the approximate formula they used for $\log L$ fails for near-critical rotation).

The comparison between the Stoeckley–Buscombe model and the observations is not straightforward, because differences between their model-atmosphere grids and ours could be responsible for the gross differences in observed and modelled line strengths. Notwithstanding this point, the *shapes* of the observed and modelled profiles are also very different. This is crucial, because Stoeckley & Buscombe's modelling procedure was concerned with matching not the line strength, but only the width of the lines at half-depth and a shape parameter, defined as the ratio of widths at (1/4)-depth and (3/4)-depth. Stoeckley & Buscombe's values for these quantities in λ4471 are $294 \pm 5\,{\rm km\,s^{-1}}$ and 1.60 ± 0.05, while the values measured from the spectrum shown in Fig. 7 are $312\,{\rm km\,s^{-1}}$ and 1.81 (estimated uncertainties $\sim 5\,{\rm km\,s^{-1}}$, 0.03), the latter figure implying a much less boxy profile than that which they attempted to reproduce. We further note that their value for $v_{\rm e}\sin i$, $337 \pm 8\,{\rm km\,s^{-1}}$, is one of the smallest reported in the literature (see references in Section 4.3), and results in model profiles that are clearly too narrow.

Although Stoeckley & Buscombe used objective, quantitative criteria in their modelling procedures, their methodology, and the observational material (stacked photographic tracings) available to them, now give rise to concern. First, as already noted, our observations are simply not in agreement with their measurements for the strong He I λ4471 line. (They also used Mg II λ4481, which is extremely weak – with a central depth ~ 2 per cent below continuum – and blended with λ4471. Correct continuum placement must therefore be crucial to their measurements of line-widths at various depths.) Secondly, not only were they not concerned with matching observed line strengths, but they also fixed the crucial parameters M_*, R, and $T_{\rm eff}$ at pre-defined values. While this may have been necessary to minimize computational requirements, it does imply that, for example, $\omega_{\rm e}/\omega_{\rm e}({\rm crit})$ and $\sin i$ cannot be independently adjusted while still matching $v_{\rm e}\sin i$, even though the line profiles have different dependencies on these two quantities.

As Stoeckley & Buscombe provided no illustrations in their paper, it is difficult to judge how good a job their models did in reproducing the overall line profiles. However, although we have not explored as large a range of differential rotation as they considered, it is certainly true that our uniform-rotation models provide a reasonable match to observations (Figs 3, 4 and 5), while models with differential rotation as large as that found by them provide a poorer match to our spectra (Fig. 7). We conclude that Stoeckley & Buscombe's claim for strong evidence of differential surface rotation must be regarded with caution, at least in the case of HD 149757.

6 ROTATIONAL CHARACTERISTICS OF ON V STARS

If the line-strength anomalies in main-sequence ON stars are a result of exceptional surface chemistry, and if that surface chemistry is the result of CNO-processed material being brought to the surface by rotationally induced mixing, we might then expect ON stars to be more numerous among the more rapid rotators. At least two factors mitigate a simple one-to-one correspondence. First, the amount of processed material mixed to the surface is a monotonically increasing function of age, with the time-scale for initial exposure a non-negligible fraction of the main-sequence lifetime ($\gtrsim$10 per cent; Heger & Langer 2000; Meynet & Maeder 2000), even for the most rapid rotators. Secondly, in general only the *projected* equatorial rotation velocity is available.[4] This means that any approach to this question must be statistical in nature.

The simplest statistical test, and the one we follow here, is to compare the distribution of projected velocities for non-supergiant ON stars with that of their morphologically normal counterparts, using a Kolmogorov–Smirnov (K–S) test. Fig. 8 shows the cumulative probability distributions of the non-supergiant ON stars for which $v_{\rm e}\sin i$ values are tabulated by Howarth et al. (1997) and of all single stars of spectral types O8–9.5 III–V, which approximately match the spectral-type distribution of the ON sample. We use spectral types as adopted by Howarth et al., except that we categorize HD 91651 and HD 191423 as ON stars (Mathys 1988; Howarth & Prinja 1989; Section 4.4.1).

By inspection, the distribution of $v_{\rm e}\sin i$ values for ON stars is immediately seen to be skewed towards larger rotational velocities than the comparison sample; some $\sim$60 per cent of normal stars have $v_{\rm e}\sin i$ values less than $100\,{\rm km\,s^{-1}}$, but only one ON star. This qualitative conclusion is quantitatively confirmed by the K–S test, which shows that the probability that the two samples were drawn from the same parent population is as small as 2.6 per cent.

This demonstrates that the stars classified as ON main sequence are, on average, more rapid rotators than their morphologically

[4] For simplicity and convenience, we have drawn no distinction in this paper between the observational quantity $v_{\rm e}\sin i$ and the true projected equatorial rotation velocity. In practice, processes in addition to rotation probably contribute significantly to the line-width (Slettebak 1956; Conti & Ebbets 1977; Howarth et al. 1997), but in the present context this is unimportant, provided such processes apply equally to ON and morphologically normal stars.

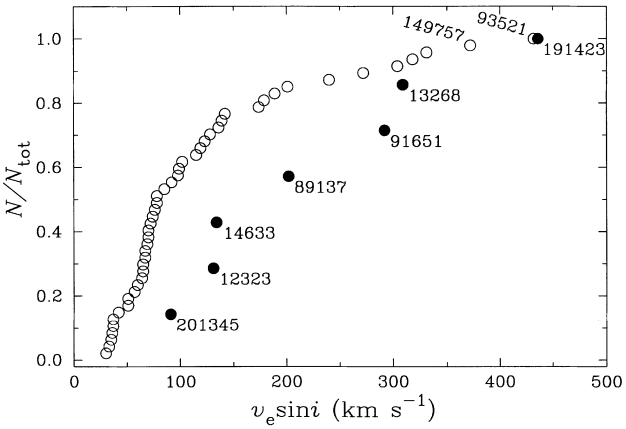

Figure 8. The cumulative probability distributions of $v_e \sin i$ for non-supergiant ON stars (filled circles) and their morphologically normal counterparts (open circles). The ON stars, together with the two additional stars analysed in this paper, are identified by their HD numbers. The differences in the cumulative distributions show that the ON stars are drawn from a more rapidly rotating population.

normal analogues. It is, however, necessary to consider this *statistical* result with caution before attaching any *physical* significance to it. First, the samples which have been compared may not be well matched: a rapidly rotating star with an apparent spectral type of ~O9 V will have a different 'intrinsic', non-rotating, spectral type, which is not accounted for in the comparison shown in Fig. 8. The effect is unlikely to exceed 1–2 subtypes (Slettebak, Kuzma & Collins 1980), and the change in maximum rotational velocity is fairly small across the range of late-O to early-B spectral types (Slettebak 1970); this effect is therefore unlikely to introduce an important bias in the comparison.

Secondly, the samples may not be 'clean', because ON characteristics become increasingly difficult to detect in classification spectra with increasing $v_e \sin i$. Indeed, of the seven ON stars identified in Fig. 8, only the three with $v_e \sin i < 150\,\mathrm{km\,s^{-1}}$ were reliably identified as morphologically N-enhanced in the era of photographic spectroscopy; the peculiarities of all four fastest rotators were overlooked by careful observers (but see Walborn 1976 and Garrison, Hiltner & Schild 1977 for comments on HD 89137 and HD 91651, respectively; Walborn's unpublished classification notes for HD 191423 also hint at ON characteristics). However, this bias, if important, would act to conceal rapidly rotating ON stars in the morphologically normal population, and thus would tend to mask the trend found here.

We conclude that ON main-sequence stars are indeed drawn from a population which possesses intrinsically more rapid rotation than morphologically normal, but otherwise physically similar, stars. The most obvious interpretation of this result is that the surface chemistry of ON stars is, at least in part, a consequence of rotationally induced mixing.

A minor caveat on this interpretation is that ON stars as a class are known to occur with high frequency in binaries (Bolton & Rogers 1978; Levato et al. 1988). We have compared our ON sample with stars which are not known to be members of binary systems because the only system with a well-established orbit in our sample is HD 12323 (Bolton & Rogers), although several other stars are suspected binaries; the morphologically normal sample will certainly also contain as yet unrecognised binaries. None the less, it does not necessarily follow directly that the ON phenomenon in main-sequence stars is causally associated with rapid rotation; it may be that both characteristics are a consequence of binarity.

7 DISCUSSION

Derived properties of the three rapid rotators analysed here are summarized in Table 1; within the observational uncertainties, these stars have identical physical characteristics. We consider HD 149757 as a specific example because its well-determined distance provides the strongest constraints on the star's physical parameters (the general discussion which follows applies to all rapid rotators we have examined); its position in the Hertzsprung–Russell diagram is shown in Fig. 9.

7.1 Surface helium abundance

Within the errors, the spectroscopic mass of HD 149757 is in agreement with the evolutionary mass ($\sim 22\,\mathrm{M_\odot}$), so there is no measurable 'mass discrepancy' for these stars. However, comparison with the latest models from the Geneva group (Meynet & Maeder 2000) does reveal a 'helium discrepancy', as those models predict essentially solar helium abundances at the observed location in the $T_{\rm eff}$, $\log g$ plane. This is because the Geneva models predict significant spin-down of the most rapid rotators during core hydrogen burning; in consequence, they imply that stars such as those considered here must be close to the zero-age main sequence (ZAMS), and such young stars have not had time to mix significant

Table 1. Summary of spectroscopically derived parameters.

	HD 93521 O9.5 V	HD 149757 O9.5 V	HD 191423 ON9 III: n	Representative uncertainty
ω_e/ω_e(crit)	0.9	0.9	0.9	+0.05, −0.10
v_e	435	425	435	±20
i (degrees)	90	70	90	±10
$T_{\rm eff}$ (kK)	33.5	34.3	34.3	±1.5
T_p (kK)	38.0	39.0	39.0	±1.5
T_e (kK)	29.9	30.7	30.7	±1.5
$\log g_p$ (dex cgs)	3.9	4.0	3.8	±0.1
$\log g_e$ (dex cgs)	3.5	3.6	3.4	±0.1
y	0.18	0.20	0.19	±0.03
$\log L$ (dex $\mathrm{L_\odot}$)	5.1	5.0	5.4	±0.5
M_* ($\mathrm{M_\odot}$)	27	20	34	±0.4 dex
R_p($\mathrm{R_\odot}$)	9.7	7.5	12.2	±0.3 dex

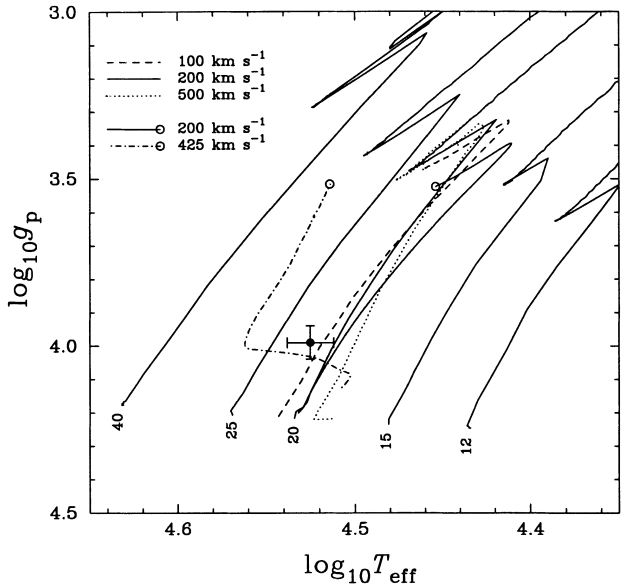

Figure 9. Evolutionary tracks in the $\log g_p$–$\log T_{eff}$ plane, labelled by initial mass (in solar masses). Different line styles correspond to different initial equatorial rotation velocities as indicated. The cross shows the observed location of HD 149757. Most tracks are from Meynet & Maeder (2000); $20\,M_\odot/200\,km\,s^{-1}$ and $20\,M_\odot/425\,km\,s^{-1}$ tracks from Heger & Langer (2000), identified by small open circles, are also included for comparison.

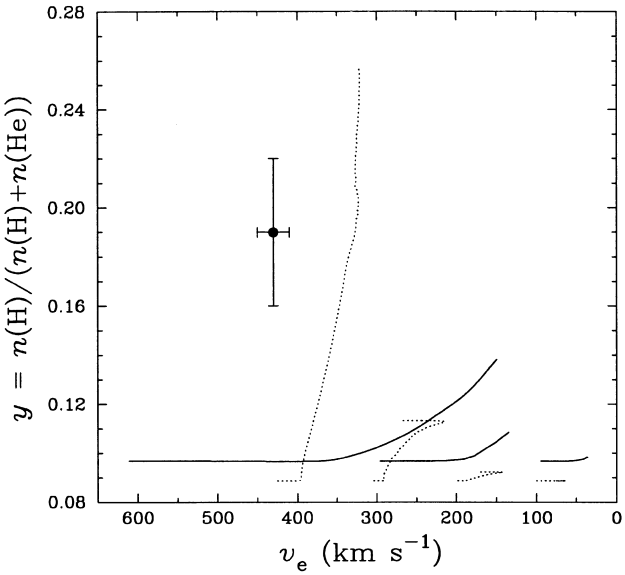

Figure 10. Surface helium abundance by number as a function of equatorial velocity during core hydrogen burning for models of 20-$M_\odot$ stars. Solid lines: Geneva models (Meynet & Maeder 2000); dotted lines: Potsdam models (Heger & Langer 2000). The initial helium abundances assumed in the two sets of models differ slightly ($Y_\odot = 0.30$, 0.28 respectively). The direction of initial evolution is always towards lower velocity and higher helium abundance, and the point with error bars illustrates the approximate properties of the rapid rotators investigated in this paper.

amounts of helium to the surface. Fig. 10 illustrates this with results from models of 20-$M_\odot$ stars with values of the initial equatorial velocity, v_{ini}, of up to 611 km s^{-1} (which is close to the critical rotation velocity for ζ Oph). For this extreme model (and for the less extreme $v_{ini} = 500\,km\,s^{-1}$ model, not illustrated), v_e decreases rapidly to the observed value of $420\,km\,s^{-1}$ after $\sim 2\times10^5$ yr, and thereafter falls more slowly to $\sim 150\,km\,s^{-1}$ by the end of core hydrogen burning, at $\sim 10^7$ yr. Only mid-way through this period does the model surface helium abundance begin to rise to levels which are observationally identifiable as non-solar, by which time v_e has fallen to $\sim 250\,km\,s^{-1}$.

At slow to moderate rotation, the calculations by Heger et al. (2000; Heger & Langer 2000), which we will refer to as Potsdam models for convenience, give similar tracks in the H-R diagram to those from the Geneva group (cf. the 20-$M_\odot$, $200\,km\,s^{-1}$ models shown in Fig. 9), although they show quasi-homogeneous evolution at less extreme rotations, as illustrated by the 20-$M_\odot$, $425\,km\,s^{-1}$ track in Fig. 9. However, the evolution of rotation in the Potsdam models is quite different, with much smaller reductions in surface equatorial velocity during core-hydrogen burning phases (Fig. 10). Coupled with quasi-homogeneous evolution for rapid rotators, which results in large surface enhancements of products of nucleosynthesis, this leads to models which match the observed characteristics of stars like HD 149757 more closely. For example, a Potsdam 20-$M_\odot$ model with $v_{ini} = 425\,km\,s^{-1}$ (model H20B of Heger et al. 2000) has $y \simeq 0.2$, $\log L \simeq 5.0\,dex\,L_\odot$, $T_{eff} \simeq 36\,kK$, and $v_e \sin i \simeq 330\,km\,s^{-1}$ at age $t \simeq 10^7$ yr, providing a reasonable approximation to the systems analysed here. More generally, homogeneously evolving models are likely to give to give better agreement with our observations than models in which the 'μ-barrier' inhibits mixing from the core (cf., for example, Maeder 1987; Beech & Mitalas 1989).

7.2 Mass loss and the evolution of angular momentum

Although the latest generation of models from both the Geneva and Potsdam groups address the effects of rotation on stellar evolution, there are important differences in the physics used in the two grids. The Potsdam models take into account a wider range of rotationally induced instabilities (cf. Heger et al. 2000), while the Geneva models use a more sophisticated (diffusive-advective) treatment of angular-momentum transport. The models also differ in many other details, of course, including the mass-loss formalisms.

The evolution of equatorial rotation in the models depends on the detailed physics used for the transport of interior angular momentum, and on the removal of angular momentum by stellar-wind mass loss. Two areas, in particular, are subject to uncertainty where the mass loss is concerned. First, the outflow is assumed to be spherically symmetric. Secondly, both the Geneva and Potsdam models assume that the stellar-wind mass-loss rate, $\dot{M}$, increases rapidly near to critical rotation:

$$\dot{M}(v_e) = \dot{M}(0)[1 - v_e/v_e(\mathrm{crit})]^\zeta, \qquad (10)$$

(Bjorkman & Cassinelli 1993), with $\zeta = -0.43$ (Potsdam) or -0.5 (Geneva).

The geometry of the outflow, which is crucial for the removal of angular momentum,[5] is not well understood in rapid rotators (e.g. Cranmer & Owocki 1995; Owocki, Cranmer & Gayley 1996;

[5] The mechanism of angular-momentum loss is not the 'Schatzman mechanism' (i.e. magnetic braking) familiar in late-type stars with outer convective zones; the removal of an outer skin of material from a radiative envelope does not of itself affect the specific angular momentum of the underlying star, although the outflow geometry does determine how much momentum is removed in total. It is the structural response of the star to the removal of material which determines the surface-rotation characteristics (cf. fig. 2 of Langer 1998), and that response depends sensitively on the treatment of internal angular momentum transport, which differs between the Potsdam and Geneva models.

Gayley & Owocki 2000). Clearly, if the surface mass flux at the poles is greater than at the equator, as in the models by Cranmer & Owocki (1995), then the angular-momentum loss is reduced compared to the spherically symmetric case, for a given global $\dot{M}$. However, under some circumstances the cooler equatorial regions may experience greater mass flux than the poles (a 'bi-stable' outflow; e.g. Vink, de Koter & Lamers 1999). In either case, the response of the evolutionary models to non-spherically symmetric mass loss is moot.

The dependence of mass-loss on rotation is not well established theoretically (although this question has recently been re-examined by Maeder & Meynet 2000a); equation (10) is based on simple 1D models by Friend & Abbott (1986), and properly applies only to the *equatorial*, not global, outflow. Nor are observational data very constraining; Howarth & Prinja (1989) found a correlation between projected rotation and column density in UV P-Cygni profiles for O-type stars, which they interpreted as indicating an increase in $\dot{M}$ with v_e, but the dispersion is large, and they arbitrarily chose simple linear functions to parametrize the data. (Those functions lead to a slower rise in $\dot{M}$ as critical rotation is approached than is suggested by equation 10.)

7.2.1 *Mass loss from HD 149757 and other O dwarfs*

The interpolation formulae used to estimate mass loss in the two sets of evolutionary grids give significantly different results for late-O main-sequence stars. Heger et al. (2000) adopt the formalism given by Nieuwenhuijzen & de Jager (1990), which for the parameters of HD 149757 yields $\dot{M} = -6.01\,\mathrm{dex\,M_\odot\,yr^{-1}}$ (to which equation 10 indicates a rotational correction of $+0.18$ dex). Meynet & Maeder (2000) use an expression from Lamers & Cassinelli (1996, hereafter LC96), which gives $\dot{M} = -8.10\,\mathrm{dex\,M_\odot\,yr^{-1}}$ (plus a rotational correction of $+0.28$ dex; this differs from the Heger et al. correction because the two groups employ different definitions of v_e(crit), as discussed in Section 7.2.2).

The fit formulae adopted in the Geneva and Potsdam models therefore predict mass-loss rates which differ by two orders of magnitude for stars such as those studied here. HD 149757 offers an opportunity to investigate this substantial discrepancy, since we can obtain a relatively precise estimate of its mass-loss rate from radio observations of stellar-wind free-free emission, using the standard Wright & Barlow (1975) formalism. The formalism assumes a spherically symmetric outflow; although this may not hold for rapid rotators, the derived mass-loss rate is insensitive to this assumption (Schmid-Burgk 1982). We further assume that the wind is not clumped in the radio-emitting region, and that the cm emission is purely thermal; if either assumption is incorrect, the inferred mass-loss rate would decrease.

Using the 3.6-cm measurement of wind emission by Howarth & Brown (1991; $S_\nu = 0.18 \pm 0.02$ mJy), a terminal velocity of $v_\infty = 1505\,\mathrm{km\,s^{-1}}$ (Howarth et al. 1997; the inferred $\dot{M}$ scales linearly with v_∞), the *Hipparcos* parallax, and our determination of the surface helium abundance, yields $\log \dot{M} = -7.18 \pm 0.08\,\mathrm{dex\,M_\odot\,yr^{-1}}$ (if helium is doubly ionized in the radio-emitting regions; -7.04 ± 0.08 if it is singly ionized), where the error reflects the uncertainty in both distance and measured flux density. We see that the two mass-loss formulae used in the evolutionary models give results which are in more or less equally poor agreement with observations of HD 149757.

A particular puzzle is that in the parameter space occupied by HD 149757 – indeed, for the greater part of the O-dwarf regime – the LC96 formula used by Meynet & Maeder (2000) is largely tied to the Howarth & Brown measurement of 3.6-cm emission from HD 149757;[6] of O-type stars with detected thermal radio emission, it is the only one significantly fainter than $\log L = 5.6\,\mathrm{dex\,L_\odot}$, and the only one with a main-sequence luminosity classification. If the fit formula given by LC96 is tied to observations of ζ Oph, why does it underestimate the observed mass-loss rate by about an order of magnitude?

The radio mass-loss rates used by LC96 came from a recalculation by Lamers & Leitherer (1993) of the mass-loss rate from Howarth & Brown (1991). Although Lamers & Leitherer adopted an absolute magnitude and luminosity, based on spectral type, which agree with *Hipparcos* values, they then used a rounded-down distance of 0.1 kpc to derive $\dot{M}$, thereby introducing a modest inconsistency between the mass-loss rate and luminosity. This inconsistency was compounded when LC96 adopted $\log L = 5.22\,\mathrm{dex\,L_\odot}$ from Puls et al. (1996), who used the pre-*Hipparcos* absolute magnitude of $M(V) = -5.1$ ($D = 0.21$ kpc) advocated by Herrero et al. (1992) on the basis of a surface-gravity determination, which they considered indicates class III luminosity. In short, the low-luminosity end of the LC96 mass-loss formalism relies heavily on results for HD 149757 which combine a mass-loss rate calculated by assuming $D = 100$ pc with a luminosity calculated by assuming $D = 210$ pc.[7] Unfortunately, this has important consequences for predicted mass-loss rates, because of the extremely steep dependence of mass loss on luminosity implied by the LC96 expression for mid- to late-O main-sequence stars: $\dot{M} \propto L^{3.2}$.

An ad hoc correction to the LC96 formula is obtained by assuming that the offset of 0.49 dex between wind momenta of supergiants and class IV/V stars of equal luminosity that they give (and which largely follows from Puls et al. 1996) is correct. Then, using the terminology of LC96, the correction factor to their equation (11), which reproduces the observations of HD 149757, is

$$C_{\mathrm{Gal}} = -0.49 - 0.17 \times [5.60 - \log(L_*)] \qquad (11)$$

(i.e. $\dot{M} \propto L^{1.7}$), if no account is taken of rotation and the terminal velocity obtained with the LC96 formulae ($v_\infty \simeq 2300\,\mathrm{km\,s^{-1}}$ for $M_* = 20\,\mathrm{M_\odot}$) is used. While this result may be more generally applicable to O dwarfs (it is in close agreement with the simple $\dot{M} \propto L^{1.7}$ dependence of O-star mass-loss given by Howarth & Prinja 1989, which predicts $\dot{M} = -7.02\,\mathrm{dex\,M_\odot\,yr^{-1}}$ for HD 149757), extrapolation to the B-dwarf regime is probably not safe.

7.2.2 *Implications for momentum loss: Potsdam models*

We have discussed the mass-loss rate of ζ Oph at some length because of the potential implications it has for the wider issue of main-sequence O-star mass-loss rates adopted in the stellar-evolution models. We conclude that the models use mass-loss rates which are probably about an order of magnitude in error for late-O main-sequence stars, if the standard assumptions we have used in

[6] This implies that rotational corrections to LC96's mass-loss rates in this part of the H–R diagram should not be applied with respect to an assumed zero-rotation baseline, as done by Meynet & Maeder (2000), but to a baseline defined by the extreme rotation of HD 149757.

[7] This appears also to explain why Vink, de Koters & Lamers (2000) obtained poor agreement between their 'observed' and 'modelled' mass-loss rates for ζ Oph. Adopting our values for T_{eff} and $\log L$ (and $M_* = 22\,\mathrm{M_\odot}$, $v_\infty/v_{\mathrm{esc}} = 2.6$) we obtain $\dot{M} = -6.86\,\mathrm{dex\,M_\odot\,yr^{-1}}$ from their fit formula. The modelled minus observed difference of 0.3 dex is consistent with the general dispersion of observations about that formula.

deriving the mass-loss rate for HD 149757 – i.e. thermal radio emission from an unclumped outflow – are valid. Paradoxically, however, while the Potsdam models use mass-loss rates for late-O dwarfs which are nearly two orders of magnitude greater than those adopted in the Geneva calculations, they none the less show a much less rapid decline in surface angular momentum. This emphasizes the key role of interior transport in determining surface properties, and the differences in modelling this transport in the two sets of grids.

The Potsdam grid includes models that are in reasonable agreement with the properties inferred here for the most rapid rotators, partly because the models predict relatively slow spin-down from the ZAMS (Fig. 10). However, this slow spin-down itself introduces a potential problem: it leads to the expectation that at the end of core hydrogen burning some O-type stars should still be rotating rather rapidly ($v_e \gtrsim 300\,\mathrm{km\,s^{-1}}$), while the most rapidly rotating O supergiants have $v_e \sin i \lesssim 200\,\mathrm{km\,s^{-1}}$ (Howarth et al. 1997; the Geneva models spin down to rotational velocities commensurate with observed values).

A further potential concern with the Potsdam models of rapid rotators is that they may encounter the Ω limit discussed by Langer (1998). The Ω limit results from a modification of the traditional Eddington limit by rotation, but it neglects von Zeipel, or gravity, darkening. The critical equatorial rotation velocity in the Ω limit is thus smaller by a factor $\sqrt{(1-\Gamma)}$ than in the Eddington limit (compare equation 2 of Langer 1998 with equation A5 of Howarth & Reid 1993), where Γ is the ratio of actual to Eddington luminosities. Consequently, imposing the Ω limit in place of the Eddington limit leads to enhanced rotationally induced mass loss (through equation 10), which can have important consequences for a star's evolution (cf., e.g. model H15B of Heger et al. 2000). However, the physical relevance of the Ω limit is far from clear; Glatzel (1998) argues that the neglect of gravity darkening is poorly justified theoretically, and in Section 3.4 we have briefly summarized the considerable observational evidence for its occurrence. This suggests that the traditional Eddington limit is more appropriate to early-type stars. In practice, this turns out to be of little importance for the stars discussed here, in spite of their rapid rotation; their Eddington factors are sufficiently small ($\lesssim$0.1) that they have rather little effect on v_e(crit), and the rotation is in any case substantially subcritical [$v_e/v_e(\mathrm{crit}) \lesssim 0.7$].

7.2.3 Implications for momentum loss: Geneva models

A possible way round the difficulty of rapid spindown in the Geneva models is offered by noting that the most rapid rotation, and hence (via equation 10) the most enhanced mass loss, is predicted at the earliest evolutionary phases. If the modelled mass-loss rates were too great near the ZAMS (even if they are too small subsequently), the modelled spin-down could be too fast, which could offer a means of reconciliation with observations. However, in the models, post-ZAMS stars evolve towards higher luminosity as well as slower rotation, and both factors enter the model mass-loss rates. To investigate this, we show results from a Maeder & Meynet (2000) $20\,\mathrm{M_\odot}$, $v_{\mathrm{ini}} = 500\,\mathrm{km\,s^{-1}}$ track in Fig. 11. For this model, the most important influence on the mass-loss rate as the star evolves is not the decrease associated with the decreasing equatorial rotation, but the increase associated with the increasing luminosity during the main sequence.

We conclude that modifications to the model angular-momentum losses through changes to the mass-loss rates alone are unlikely to reconcile the Geneva evolutionary calculations with the observation that very rapidly rotating late-O main-sequence stars seem to exhibit enhanced surface helium abundances. Because the models apparently lose angular momentum too rapidly compared with observations, while at the same time underestimating the actual mass-loss rates by a factor ~ 10, it is unlikely that dropping the models' assumption of spherically symmetric mass loss will substantially alter this conclusion. None the less, in this context it would clearly be worth exploring the possibility that most mass is lost through polar outflows in rapid rotators, as suggested by Cranmer & Owocki (1995) and Maeder (1999).

Finally we recall that, in observing the photosphere, we measure rotation in only the very outermost layer of the star, which has negligible mass. Thus simplifications in the treatment of angular-momentum transport which are unimportant for global stellar properties may have important consequences for the observed rotation. Moreover, the diffusion coefficients employed in the evolutionary models to characterize both the mixing of material and the transport of angular momentum may be inaccurate; there are no first-principles expressions for either D_h or D_v, the horizontal and vertical components of turbulent diffusion. The expression for D_h proposed by Zahn (1992) is described by him as 'unavoidably crude', but we may hope that observations such as those presented here may offer constraints on its value. For now, it remains unclear how much angular momentum is transferred to the stellar atmosphere by meridional circulation, and how much by turbulent diffusion (Denissenkov et al. 1999).

7.3 Binary evolution?

The foregoing discussion is based on the assumption that the observed spectral characteristics arise as a consequence of single-star evolution. This assumption is justified only to the extent that none of the rapid rotators discussed here is known to show convincing evidence for a binary companion. However, HD 149757 is a well-known 'runaway star' (e.g. Blaauw 1961), and there is good evidence that its space motion may be the consequence of a supernova explosion in a former close binary companion, ~ 1 Myr ago, which disrupted the system (Hoogerwerf, de Bruijne & de Zeeuw 2001). Both HD 93521 and HD 191423 have also been classified as runaways, although on somewhat weaker grounds (Gies 1987; Howarth et al. 1997).

If it is the case that these stars have been ejected from former close binary systems, then it may well be that both their rotational characteristics and surface chemistry are in fact the result of binary evolution (Blaauw 1993). Unfortunately, detailed predictions for this mode of evolution are not yet available, although Packet (1981) provides calculations which suggest the importance of spin-up through accretion.

7.4 CNO spectra and helium enhancements

If abundance anomalies in early-type stars result from internally CNO-processed material of initially $\sim$solar composition being mixed to the surface, then it is practically inescapable that detectable helium enhancements should be accompanied by a substantial increase in the nitrogen:carbon ratio, regardless of the processes producing the mixing. This qualititative statement is quantitatively supported by all recent evolutionary models, which show that the relative change in N:C ratio is much larger than that in helium abundance, irrespective of differences in detailed physics (e.g. Heger & Langer 2000; Meynet & Maeder 2000).

At least one BN supergiant is reported to show an enhanced

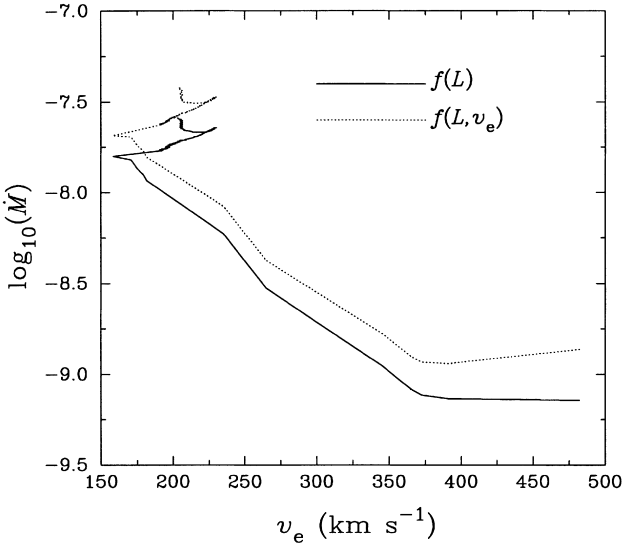

Figure 11. Modelled mass-loss rates (in solar masses per year) as a function of equatorial rotation velocity for a 20-$M_\odot$ model with $v_{\rm ini} = 500\,{\rm km\,s^{-1}}$ (from Meynet & Maeder 2000), with and without a correction for rotation (equation 10). The mass-loss rate is expected to decrease with decreasing $v_{\rm e}$ as the star evolves from the ZAMS (i.e. away from the lower right in this diagram); although this does occur at the very earliest stages for the rotationally corrected mass-loss rates, the effect is relatively small, and is overwhelmed by the effect of increasing luminosity for the greater part of the tracks. Note that all the mass-loss rates are probably too small, as discussed in Section 7.2.1.

surface nitrogen abundance, accompanied by depleted carbon and oxygen, but with solar helium: the peculiar binary HD 163181 (Kane, McKeith & Dufton 1981). This might lead one to expect clear evidence of enhanced nitrogen abundances wherever a helium enhancement is detectable. However, not all stars for which enhanced helium abundances are inferred necessarily show anomalous characteristics in their CNO spectra, even at spectral types where such anomalies are detectable in classification spectra with relative ease ($\sim$ O9–B1). For supergiants, this may be because the majority of stars – which define morphological normalcy – already exhibit enhancements in *both* surface helium abundance and N:C ratio; the OBC supergiants are then those relatively rare objects with near-solar surface abundances, while in OBN supergiants mixing has proceeded to the greatest extent (Walborn 1976, 1988; Smith & Howarth 1994).

As expected, ON characteristics in main-sequence stars also appear to be associated with enhanced surface helium abundance (Schönberner et al. 1988; HD 191423, Section 4.4). Until now, the presumed corollary has been that morphologically normal late-O main-sequence stars have near-solar surface chemistry, in respect of both helium and CNO. However, our spectroscopic analyses of HD 93521 and HD 149757 confirm previous suggestions of enhanced surface helium abundances in these stars (Hack & Yilmaz 1977, Lennon et al. 1991; Herrero et al. 1992, Puls et al. 1996), and put such suggestions on a more secure footing by taking into account the variations in temperature and gravity across the surfaces of these rapid rotators. Both these stars have morphologically normal CNO spectra, in a spectral domain where anomalous spectra may be identified reasonably easily (Fig. 6). At least one of the following must therefore be true: (i) an unknown mechanism permits surface helium enhancements without accompanying changes in the N:C ratio; (ii) our spectroscopic determinations of y are flawed (along with similar determinations by previous authors); (iii) spectral morphology does not reliably track surface chemistry.

We will not comment further on option (i). Option (ii) is certainly possible, given the obvious deficiencies of plane-parallel, hydrostatic, non-LTE H/He model atmospheres such as those used here, which are believed to tend to yield gravities which are too low and temperatures which are too high. However, models of this nature appear to show no obvious bias towards systematic overestimation of helium abundances, at least not near the main sequence, as they can yield solar values across much of the $T_{\rm eff}$, $\log g$ domain of interest (e.g. Schönberner et al. 1988; Herrero et al. 1992, 1999; Section 4.1). Moreover, the same models show no significant differences in helium abundance between the ON star HD 191423 and the two morphologically normal rapid rotators studied here – in other words, if the helium-abundance analysis fails, it fails both absolutely *and* differentially.

Option (iii) is, therefore, perhaps the most plausible interpretation at present, in view of the strong sensitivity of the classification lines to luminosity and temperature. Mathys (1988), in a careful review of quantified morphological characteristics of late-O stars, has already concluded that some stars in this spectral range may have enhanced surface nitrogen abundances compared to objects with similar spectral classifications. However, the situation in respect of the CNO spectra must be regarded as unresolved until such time as more elaborate models allow reliable determinations of the light-metal abundances.

8 CONCLUSIONS

(i) We have conducted a fine analysis of three rapidly rotating late-O stars (together with a narrow-lined control star) by using plane-parallel, hydrostatic, H/He non-LTE models. The models account for the variations in temperature and gravity across the stellar surface expected from von Zeipel's 'law', for which we summarize supporting observational evidence (Section 3.4). For all three stars, we find $y \simeq 0.2$ (Section 4).

(ii) Although binary evolution cannot be ruled out as a factor (Sections 6 and 7.3), rotationally induced mixing is the obvious qualitative interpretation of the enhanced surface helium abundance. Quantitatively, the pairing of very rapid rotation with very high helium abundances is not consistent with the latest generation of Geneva models. To investigate this problem we have examined the question of mass loss for stars such as those we have studied. We have shown that the mass-loss rates for O dwarfs used in the Geneva models are too small; however, correcting this problem is unlikely to bring the models into agreement with the atmospheric analysis (Section 7.1). The Potsdam models employ mass-loss rates which are too large, but none the less retain rapid rotation at later core-hydrogen-burning stages; this alleviates the rotation/helium problem, but suggests that larger numbers of rapidly rotating O supergiants should be present than are actually detected.

(iii) Although high surface-helium abundances are derived for all three stars, only one of them shows the spectral morphology of a classical ON star (demonstrated here for the first time). This presents an anomaly, because helium and nitrogen enhancements are expected to go hand-in-hand. If the helium analysis is in error (i.e. if the atmospheric models used here are inadequate for the determination of y), it is unclear why it should yield indistinguishable results for the physically similar O-normal and ON stars analysed here (in other words, why it should not succeed at least differentially), or why the methods used here should

successfully yield solar helium abundances for many stars (Section 7.4). If the helium analysis is correct, it raises the spectre that spectral morphology of CNO features may not track surface chemical abundances faithfully; there is some evidence, albeit weak, in favour of this interpretation (Section 7.4).

(iv) ON main-sequence stars are drawn from a more rapidly rotating population than morphologically normal stars are; this is a robust result insofar as it is independent of models. If we accept that, in general, ON morphology indicates the presence of processed material in the photosphere, then this result provides a strong qualitative indication of the importance of rotationally induced mixing (Section 6).

(v) Our model spectra are not consistent with strongly differential surface rotation previously suggested; uniform ('shellular') surface rotation provides a satisfactory match between models and observations (Section 5).

(vi) The absolute magnitudes and masses of rapid rotators can be found from their spectra alone, albeit with rather low precision (Section 3.6). In this way, we confirm that HD 93521 is a Population I star at ~ 2 kpc (Section 4.2).

ACKNOWLEDGMENTS

When most of the observations reported here were obtained, the William Herschel Telescope was operated on the island of La Palma by the Royal Greenwich Observatory at the Spanish Observatorio del Roque de los Muchachos of the Instituto de Astrofisica de Canarias. This research was, in addition, partially based on data from the ING archive. We thank Ivan Hubeny for provision and support of TLUSTY, and Georges Meynet and Alex Heger for results from the Geneva and Potsdam stellar-evolution models. Useful suggestions and comments on an early draft were made by Norbert Langer, Georges Meynet, Nolan Walborn, Jorick Vink, and André Maeder, who, as referee, additionally contributed helpful remarks on the final version.

REFERENCES

Balona L., Kambe E., 1999, MNRAS, 308, 1117
Becker S. R., Butler K., 1989, A&A, 209, 244
Beech M., Mitalas R., 1989, A&A, 213, 127
Bisiacchi B. F., Lopez J. A., Firmani C., 1982, A&A, 107, 252
Bjorkman J. E., Cassinelli J. P., 1993, ApJ, 409, 429
Bjorkman J. E., Ignace R., Tripp T. M., Cassinelli J. P., 1994, ApJ, 435, 416
Blaauw A., 1961, Bull. Astron. Inst. Netherlands, 15, 265
Blaauw A., 1993, in Cassinelli J. P., Churchwell E. B., eds, ASP Conf. Ser. Vol. 35, Massive Stars: Their Lives in the Interstellar Medium. Astron. Soc. Pac., San Francisco, p. 207
Bolton C. T., Rogers G. L., 1978, ApJ, 222, 234
Collins G. W., II, 1963, ApJ, 138, 1134
Collins G. W., II, Harrington J. P., 1966, ApJ, 146, 152
Conti P. S., Ebbets D. C., 1977, ApJ, 213, 438
Cranmer S. R., Owocki S. P., 1995, ApJ, 440, 308
Denissenkov P. A., Ivanova N. S., Weiss A., 1999, A&A, 341, 181
Ebbets D. C., 1981, PASP, 93, 119
Ebbets D. C., Savage B. D., 1982, ApJ, 262, 234
ESA, 1997, The Hipparcos and Tycho Catalogues. ESA, Noordwijk (ESA-SP1200)
Fliegner J., Langer N., Venn K. A., 1996, A&A, 308, L13
Friend D. B., Abbott D. C., 1986, ApJ, 311, 701
Fullerton A. W., Gies D. R., Bolton C. T., 1991, BAAS, 23, 1379
Garrison R. F., Hiltner W. A., Schild R. E., 1977, ApJS, 35, 111
Gayley K. G., Owocki S. P., 2000, ApJ, 537, 461
Gies D. R., 1987, ApJS, 64, 545
Gies D. R., Lambert D. L., 1992, ApJ, 387, 673
Glatzel W., 1998, A&A, 339, L5
Grigsby J. A., Morrison N. D., Anderson L. S., 1992, ApJS, 78, 205
Hack M., Yilmaz N., 1977, Ap&SS, 48, 483
Hanbury Brown R., Davis J., Allen L. R., 1974, MNRAS, 167, 121
Hardorp J., Strittmatter P. A., 1968, ApJ, 153, 465
Heger A., Langer N., 2000, ApJ, 544, 1016
Heger A., Langer N., Woosley S. E., 2000, ApJ, 528, 368
Herrero A., Kudritrzki R. P., Vilchez J. M., Kunze E., Butler K., Haser S., 1992, A&A, 261, 209
Herrero A., Corral L. J., Villamariz M. R., Martín E. L., 1999, A&A, 348, 542
Herrero A., Puls J., Villamariz M. R., 2000, A&A, 354, 193
Hobbs L. M., Morgan W. W., Alber C. E., Lockman F. J., 1982, ApJ, 263, 690
Hoogerwerf R., de Bruijne J. H. J., de Zeeuw P. T., 2001, A&A
Howarth I. D., 1997, Observatory, 117, 335
Howarth I. D., Brown A. B., 1991, in van der Hucht A., Hidayat B., eds, Proc. IAU Symp. 143, Wolf-Rayet Stars and Interrelations with Other Massive Stars in Galaxies. Kluwer, Dordrecht, p. 315
Howarth I. D., Prinja R. K., 1989, ApJS, 69, 527
Howarth I. D., Reid A. H. N., 1993, A&A, 279, 148
Howarth I. D. et al., 1993, ApJ, 417, 338
Howarth I. D., Siebert K. W., Hussain G. A. J., Prinja R. K., 1997, MNRAS, 284, 265
Hubeny I., Lanz T., 1995, ApJ, 439, 875
Hubeny I., Heap S. R., Lanz T., 1998, in Howarth I., ed., ASP Conf. Ser. Vol. 131, Boulder-Munich II: Properties of Hot, Luminous Stars. Astron. Soc. Pac., San Francisco, p. 108
Irvine N. J., 1989, ApJ, 337, L33
Jankov S., Janot-Pacheco E., Leister N. V., 2000, ApJ, 540, 535
Kambe E. et al., 1997, ApJ, 481, 406
Kane L. G., McKeith C. D., Dufton P. L., 1981, MNRAS, 194, 537
Kippenhahn R., Weigert A., 1990, Stellar Structure and Evolution. Springer-Verlag, Berlin, p. 436
Kudritzki R. P., Hummer D. G., Pauldrach A. W. A., Puls J., Najarro F., Imhoff J., 1992, A&A, 257, 655
Lamers H. J. G. L. M., Cassinelli J. P., 1996, in Leitherer C., Fritze-von Alvensleben U., Huchra J., eds, ASP Conf. Ser. Vol. 98, From Stars to Galaxies: The Impact of Stellar Physics on Galaxy Evolution. Astron. Soc. Pac., San Francisco, p. 162 (LC96)
Lamers H. J. G. L. M., Leitherer C., 1993, ApJ, 412, 771
Lamers H. J. G. L. M., Vink J. S., de Koter A., Cassinelli J. P., 1999, in Wolf B., Stahl O., Fullerton A. W., eds, Proc. IAU Symp. 169, Lecture Notes in Physics 523, Variable and Non-spherical Stellar Winds in Luminous Hot Stars. Springer-Verlag, Berlin, p. 159
Langer N., 1998, A&A, 329, 551
Lennon D. J., 1994, Space Sci Rev., 66, 127
Lennon D. J., Dufton P. L., Keenan F. P., Holmgren D. E., 1991, A&A, 246, 175
Levato H., Morrell N., Garcia B., Malaroda S., 1988, ApJS, 68, 319
McErlean N. D., Lennon D. J., Dufton P. L., 1998, A&A, 329, 613
Maeder A., 1998, in Howarth I., ed., ASP Conf. Ser. Vol. 131, Boulder-Munich II: Properties of Hot, Luminous Stars. Astron. Soc. Pac., San Francisco, p. 85
Maeder A., 1987, A&A, 178, 159
Maeder A., 1999, A&A, 347, 185
Maeder A., Meynet G., 2000a, A&A, 361, 159
Maeder A., Meynet G., 2000b, ARA&A, 38, 143
Martin P. G., 1970, Ap&SS, 1, 119
Massa D., 1992, in Drissen L., Leitherer C., Nota A., eds, ASP Conf. Ser. Vol. 22, Nonisotropic and Variable Outflows from Stars. Astron. Soc. Pac., San Francisco, p. 84
Massa D., 1995, ApJ, 438, 376
Mathys G., 1988, A&AS, 76, 427
Meynet G., Maeder A., 1997, A&A, 321, 465
Meynet G., Maeder A., 2000, A&A, 361, 101

Mills D., Webb J., Clayton M., 1997, Starlink User Note 152.4. Rutherford Appleton Laboratory, Didcot, Oxon
Moffett T. J., Barnes T. G., III, 1979, PASP, 91, 180
Morgan W. W., Code A. D., Whitford A. E., 1955, ApJS, 2, 41
Nieuwenhuijzen H., de Jager C., 1990, A&A, 231, 134
Owocki S. P., Cranmer S. R., Gayley K. G., 1996, ApJ, 472, L115
Packet W., 1981, A&A, 102, 17
Penny L. R., 1996, ApJ, 463, 737
Plavec M., 1958, Mem. Soc. R. Sci. Liège, 20, 411
Porter J. M., 1996, MNRAS, 280, L31
Puls J. et al., 1996, A&A, 305, 171
Rafert J. B., Twigg L. W., 1980, MNRAS, 193, 79
Reid A. H. N. et al., 1993, ApJ, 417, 320
Schaller G., Schaerer D., Meynet G., Maeder A., 1992, A&AS, 96, 269
Schmid-Burgk J., 1982, A&A, 108, 169
Schönberner D., Herrero A., Becker S., Eber F., Butler K., Kudritzki R. P., Simon K. P., 1988, A&A, 197, 208
Slettebak A., 1956, ApJ, 124, 173
Slettebak A., 1966, ApJ, 145, 126
Slettebak A., 1970, in Slettebak A., ed., Stellar Rotation. Reidel, Dordrecht, p. 3
Slettebak A., Kuzma T. J., Collins G. W., II, 1980, ApJ, 242, 171
Smith K. C., Howarth I. D., 1994, MNRAS, 290, 868
Smith K. C., Howarth I. D., 1998, MNRAS, 299, 1146
Stoeckley T. R., 1968, MNRAS, 140, 121
Stoeckley T. R., Buscombe W., 1987, MNRAS, 227, 801
Villamariz M. R., Herrero A., 2000, A&A, 357, 597
Vink J. S., de Koter A., Lamers H. J. G. L. M., 1999, A&A, 350, 181
Vink J. S., de Koter A., Lamers H. J. G. L. M., 2000, A&A, 362, 295
Voels S. A., Bohannan B., Abbott D. C., Hummer D. G., 1989, ApJ, 340, 1073
Vogt S. S., Penrod G. D., 1983, ApJ, 275, 661
von Zeipel H., 1924, MNRAS, 84, 665
Walborn N. R., 1973, AJ, 78, 1067
Walborn N. R., 1976, ApJ, 205, 419
Walborn N. R., 1988, in Nomoto K., ed., Proc. IAU Symp. 108, Lecture Notes in Physics 305, Atmospheric Diagnostics of Stellar Evolution: Chemical Peculiarity, Mass Loss, and Explosion. Springer-Verlag, Berlin, p. 70
Wallerstein G., Wolff S. C., 1965, PASP, 77, 12
Wright A. E., Barlow M. J., 1975, MNRAS, 170, 41
Zahn J.-P., 1992, A&A, 265, 115

This paper has been typeset from a TEX/LATEX file prepared by the author.